PB-244 922

A PREDICTIVE MODEL FOR TRANSIENT TEMPERATURE DISTRIBUTIONS IN UNSTEADY FLOWS

Donald R. F. Harleman, et al

Massachusetts Institute of Technology

Prepared for:

National Environmental Research Center

November 1973

DISTRIBUTED BY:

NTIS

National Technical Information Service
U. S. DEPARTMENT OF COMMERCE

R74-5 267037 PB 244 922

A PREDICTIVE MODEL FOR TRANSIENT TEMPERATURE DISTRIBUTIONS IN UNSTEADY FLOWS

by

Donald R. F. Harleman

Dominique N. Brocard

and

Tavit O. Najarian

RALPH M. PARSONS LABORATORY
FOR WATER RESOURCES AND HYDRODYNAMICS

Report No. 175

Prepared with the support of
National Coastal Pollution Research Program
(Grant No. R800429)
National Environmental Research Center
U. S. Environmental Protection Agency
Corvallis, Oregon
in cooperation with
Environmental Devices Corporation
Marion, Massachusetts
and
Philadelphia Electric Company
Philadelphia, Pennsylvania

November 1973

Reproduced by
NATIONAL TECHNICAL
INFORMATION SERVICE
U.S. Department of Commerce
Springfield, VA. 22151

MIT

DEPARTMENT
OF
CIVIL
ENGINEERING

SCHOOL OF ENGINEERING
MASSACHUSETTS INSTITUTE OF TECHNOLOGY
Cambridge, Massachusetts 02139

PB244922

BIBLIOGRAPHIC DATA SHEET	1. Report No. 175	2.	3. Recipient's Accession No.
4. Title and Subtitle A predictive model for transient temperature distributions in unsteady flows.			5. Report Date Nov. 1973
			6.
7. Author(s) Donald R. F. Harleman, Dominique N. Brocard, Tavit O. Najarian			8. Performing Organization Rept. No.
9. Performing Organization Name and Address Dept. of Civil Engineering Massachusetts Institute of Technology Boston, Mass			10. Project/Task/Work Unit No.
			11. ~~Contract~~/Grant No. R 800429
12. Sponsoring Organization Name and Address Nat'l. Environmental Research Center U.S. Environmental Protection Agency Corvallis, Oregon			13. Type of Report & Period Covered
			14.

15. Supplementary Notes

16. Abstracts This report is part of a continuing program to develop mathematical models for interacting water quality parameters in unsteady flows. Because of the temperature dependance of biochemical rate constants, it is important to have a method of predicting transient water temperature distributions under varying meteorological conditions with or without heat inputs from electric power generating stations

17. Key Words and Document Analysis. 17a. Descriptors

* Water quality
* Mathematical models
* temperature distribution
* water flow

17b. Identifiers/Open-Ended Terms

17c. COSATI Field Group

PRICES SUBJECT TO CHANGE

18. Availability Statement	19. Security Class (This Report)	21. No. of Pages
Release unlimited	UNCLASSIFIED	106
	20. Security Class (This Page) UNCLASSIFIED	22. Price 5.25-2.25

R74-5

DSR 81016
DSR 81271

RALPH M. PARSONS LABORATORY

FOR WATER RESOURCES AND HYDRODYNAMICS

Department of Civil Engineering

Massachusetts Institute of Technology

A PREDICTIVE MODEL FOR TRANSIENT TEMPERATURE DISTRIBUTIONS IN UNSTEADY FLOWS

by

Donald R. F. Harleman

Dominique N. Brocard

and

Tavit O. Najarian

Report No. 175

November 1973

Prepared with the support of

National Coastal Pollution Research Program (Grant No. R800429)

National Environmental Research Center

U. S. Environmental Protection Agency

Corvallis, Oregon

in cooperation with

Environmental Devices Corporation

Marion, Massachusetts

and

Philadelphia Electric Company

Philadelphia, Pennsylvania

ABSTRACT

This report is part of a continuing program to develop mathematical models for interacting water quality parameters in unsteady flows. Because of the temperature dependence of biochemical rate constants it is important to have a method of predicting transient water temperature distributions under varying meteorological conditions with or without heat inputs from electric power generating stations.

The factors contributing to the heat exchange across the free surface of a body of water are reviewed and quantitative relationships for the calculation of the heat fluxes are summarized. Mathematical models are developed to determine the temperature distribution in natural bodies of water:

- A one-dimensional steady model in which the temperature distribution is a function of longitudinal distance. This model is used to show that, when the longitudinal variation of water temperatures is small (up to 10°F), the influence of the water surface temperature variation on the widely used surface heat transfer coefficient can be neglected. A sensitivity analysis is performed on the various meteorological parameters involved which shows that the most important are the relative humidity, the net radiated flux and the ambient temperature.

- A one-dimensional unsteady model in which the temperature distribution is a function of longitudinal distance and time. The flow is unsteady and non-uniform and meteorological conditions and boundary conditions are functions of time. The mathematical model is a modified version of the Dailey and Harleman (1972) transient water quality model. The model is applicable to tidal flows in estuaries and in reservoirs in which unsteady flow and flow reversals occur due to the transient operation of hydroelectric power stations at the reservoir boundaries.

Predicted temperatures from the unsteady model are compared with measurements of natural water temperatures in Conowingo Reservoir during various periods of time in April and September 1972. Additional runs were made to simulate the effect on the reservoir of heat input from Unit No. 2 of the Peach Bottom Atomic Power Station under the hypothetical condition that the heated condenser water discharge is fully mixed at the reservoir cross-section adjacent to the plant.

ACKNOWLEDGEMENTS

Primary support for this study came from the U.S. Environmental Protection Agency, Grant No. R-800429, under the project "Tidal Variation of Water Quality Parameters in Estuaries" (DSR 81016). This program is administered under the National Coastal Pollution Research Program, National Environmental Research Center, Corvallis, Oregon, by Richard J. Callaway, Project Director.

Additional support and field data for the case study of Conowingo Reservoir was provided by Environmental Devices Corporation of Marion, Mass. and Philadelphia Electric Company (DSR 81271). The cooperation of Edward C. Brainard, II, President of Environmental Devices Corporation and Miss Cecily Viall is gratefully acknowledged.

Administrative and technical supervision at M.I.T. was provided by Dr. D.R.F. Harleman, Professor of Civil Engineering and Director of the R.M. Parsons Laboratory for Water Resources and Hydrodynamics. Model development and calculations for the temperature distributions were carried out by Dominique N. Brocard, Research Assistant. Much of the material contained in this report was submitted by Mr. Brocard in partial fulfillment of the requirement for the degree of Master of Science in Civil Engineering. During a portion of this study, Mr. Brocard was supported by a fellowship of the General Electric Foundation.

Model development and calculations of the unsteady flows in Conowingo Reservoir were carried out by Tavit O. Najarian, Research Assistant. Computer work was performed at the M.I.T. Information Processing Center. Miss Kathleen Emperor typed the manuscript.

TABLE OF CONTENTS

	Page
Title page	1
Abstract	2
Acknowledgement	3
Table of contents	4
List of Figures	6
List of Tables	8
I. INTRODUCTION	9
1.1 Mathematical models for thermal pollution	9
1.2 Summary of the present study	10
II. BASIC EQUATIONS AND NEW APPROACH	12
2.1 One-dimensional models	12
2.2 Net surface flux: ϕ_n	15
2.2.1 Short wave solar radiation: ϕ_{sn}	17
2.2.2 Longwave atmospheric radiation	17
2.2.3 Longwave radiation from the water surface	20
2.2.4 Evaporative flux	20
2.2.5 Conduction heat flux: ϕ_c	25
2.2.6 Net surface flux: ϕ_n	25
2.2.7 Equilibrium temperature concept	27
2.2.8 Linearization of the net heat flux equation	28
2.3 Transformation of the heat transfer equation	29

	Page
III. STEADY STATE MODEL	33
3.1 Hypotheses	33
3.2 Possible applications	33
3.3 Development of the model	34
3.4 Sensitivity analysis	47
IV. UNSTEADY MODEL	57
4.1 Description of Dailey and Harleman's model	57
4.2 Modification of Dailey and Harleman's model	69
4.3 Test run	73
V. CASE STUDY: CONOWINGO RESERVOIR	77
5.1 Natural temperature distributions	77
5.2 Effect of waste heat input	83
VI. CONCLUSION	99
LIST OF REFERENCES	101
APPENDIX A. Summary of integral values in the weighted residual equation	102

LIST OF FIGURES

FIGURE	TITLE	PAGE
2-1	Heat transfer mechanisms at the water surface	16
2-2	Evaporative flux versus surface temperature	26
2-3	Net surface flux versus temperature	29
3-1	Position of ξ_i in the interval $[x_i, x_{i+1}]$	37
3-2	Approximation of the solution in the most unfavorable case	39
3-3	Sample run of the steady model with and without heat discharge at x = 0	46
3-4	Approximate range of variation of the corrolation coefficient for relative humidity	52
3-5	Approximate range of variation of the corrolation coefficient for the net radiated flux	53
3-6	Approximate range of variation of the corrolation coefficient for the wind velocity	54
3-7	Approximate range of variation of the corrolation coefficient for ambiant temperature	55
3-8	Approximate range of variation of the corrolation coefficient for atmospheric pressure	56
4-1	Schematic diagram of a typical estuary with multiple waste inputs	59
4-2	Definition of the interpolating funtion ϕ_j	62
4-3	Test run with steady river parameters and meteorological conditions	76
5-1	Map of the Conowingo Reservoir showing the schematization used for the model	78
5-2	Time variations of the velocity from September 1st to 3rd, 1972 at two locations in Conowingo Reservoir	85

FIGURE	TITLE	PAGE
5-3	Time variations of the temperature from September 1st to 3rd, 1972 at the upstream end of Conowingo Reservoir	86
5-4	Time variations of the temperature from September 1st to 3rd, 1972 at x = 19,000 ft. in Conowingo Reservoir	87
5-5	Time variations of the temperature from September 1st to 3rd, 1972 at x = 27,500 ft. in Conwingo Reservoir	88
5-6	Temperature profile in reach 1 of Conowingo Reservoir on September 1st, 1972 at 24 hours	89
5-7	Temperature profile in reach 1 of Conowingo Reservoir on September 2nd, 1972 at 24 hours with $E_L = 100\ E_T$	90
5-8	Temperature profile in reach 1 of the Conowingo Reservoir on September 2nd, 1972 at 24 hours with $E_L = 10\ E_T$	91
5-9	Time variations of the velocity from April 8 to 25, 1972 at x = 13,000 ft. in Conowingo Reservoir	92
5-10	Time variations of the velocity from April 8 to 25, 1972 at x = 25,000 ft. in Conowingo Reservoir	93
5-11	Time variations of the temperature from April 8 to 18, 1972 at x = 25,000 ft. in Conowingo Reservoir	94
5-12	Longitudinal temperature profile in Conowingo Reservoir on April 10, 1972 at 12 hours	95
5-13	Temperature profile in Conowingo Reservoir on April 12, 1972 at 12 hours	96
5-14	Computed excess temperature profiles in the Conowingo Reservoir due to Peach Bottom - Unit 2 with meteorological and hydrological data of April 14, 1972	97
5-15	Computed excess temperature profiles in the Conowingo Reservoir due to Peach Bottom - Unit 2 with meteorological and hydrological data of September 3, 1972	98

LIST OF TABLES

TABLE	TITLE	PAGE
2-1	Ratio of reflected to incident solar radiation	17
3-1	Reproduction of the computer output for the steady model sample run without heat discharge	42
3-2	Reproduction of the computer output for the steady model sample run with heat discharge at x = 0	44
3-3	Comparison of the temperature excess ($T - T_N$) with constant and varying K	48

I. INTRODUCTION

1.1 Mathematical Models for Thermal Discharges

Even though the dangers of a continuous growth in every domain and in energy consumption in particular are now beginning to be realized, no leveling off seems possible nor is expected for the next two decades. This means, according to the most conservative estimates, a doubling of the energy consumption between 1971 and 1990 and a tripling of the portion thereof devoted to electrical generation.

Since energy conversion is always achieved with an efficiency less 100%, a certain amount of non-convertible heat is released to the enviornment in the course of electricity production. For fossil fuel plants which have an overall thermal efficiency of approximately 40% and in-plant and stack losses of the order of 15% of the fuel heat content, the amount of condenser waste heat is about 112% of the net power production. For nuclear power plants both BWR and PWR, which have a lower efficiency (32%) and less in-plant losses (5%), the wast heat reaches 200% of the electrical output; that is 60 to 70% more than for fossil fuel plants. For each MW electrical output almost 2 MW are released to the environment as heat. Then the expected increase in the share of nuclear energy for electricity production together with the expected increase in the total electricity production raises more acutely the problem of waste heat disposal.

In order for ecological effects to be predicted when a direct waste heat discharge is envisaged in a natural body of water, a model either physical or mathematical, has to be used to determine the temperature changes that will follow. Nearer to the concern of the power plant designer is

whether the environmental control requirements will be met or not. In that case also a predictive model has to be used.

1.2 Summary of the Present Study

This study is concerned with one-dimensional models in which the computed characteristic is a cross-section averaged value. The basis of this study is a model developed by Dailey and Harleman (1972) for transient water quality in estuary networks which can be applied to any type of unsteady free surface flow. This model solves in a first step the continuity and momentum equations which govern the flow. The flow characteristics are then introduced to a mass transport type equation which is solved by the finite element techniques. Two boundary conditions have to be specified as well as an initial condition in order to obtain a unique solution to this second order partial differential equation. These boundary conditions can be either the advective or the dispersive flux of substance (or heat) across both upper and lower boundaries. Although an initial condition is required, it has been shown that an exact value is not necessary since self-adjustment occurs after a certain time.

This model has been modified here to account for some of the most recent developments in the study of heat transfer across a free water surface introduced by Ryan and Harleman (1973). Because the model treats unsteady flows, as in estuaries, the hypothesis of a constant surface heat decay coefficient and equilibrium temperature can lead to large errors, especially when the maximum temperature variation in the stream portion under study is high and when the period of time during which the model is run is long.

First a steady state, varying cross-section model was developed to study the influence of the water surface temperature on the heat decay coefficient. This model can also be applied when the river discharge is steady by averaging the meteorological conditions over a period of time (a month for instance).

These heat transfer elements were then introduced in the transient model which was tested on the Conowingo Reservoir, Pa., where the required meteorological data was available.

II. BASIC EQUATIONS AND NEW APPROACH

2.1 One-Dimensional Models

In whatever situation it is to be found, a fluid, and water in particular, always has a 3-dimensional geometry. Though, in certain circumstances, it is possible to restrict the analysis of one of its spatial characteristics -- velocity, density, temperature, etc. -- to 2 or 1 dimensions. This is the case when a direct relationship is known which enables the determination of the studied characteristic in the other 1 or 2 dimensions respectively. For instance, in a plane flow, if the velocity field is determined in the x-y plane it is also known at any other point in space through a relation of the type $\vec{u}(x,y,z) = f[\vec{u}(x,y),z]$, the most simple one being equality: $\vec{u}(x,y,z) = \vec{u}(x,y)$. This actually means that, through additional relationships, the basic vectorial equation governing the studied characteristic can be made equivalent to a set of real equations, 1 or 2 of which being solvable without the remaining ones.

This is not exactly what is done in what is being called here a 1-dimensional model. In those models, a cross-section averaged value is taken in the plane perpendicular to a privileged direction and the basic equations are transformed to include only this average value. The main difference is that it is usually not directly possible to determine the exact value of the studied characteristic, which here is temperature, at one particular point, once the average value is known. Of course such a procedure is only applicable when a privileged direction exists such as in rivers and estuaries, and when the concern is primarily in the distribution of the characteristic along this direction and not perpendicular

to it. In a stream the centerline is chosen as privileged direction.

One-dimensional models have the advantage of simplicity and they require less data input than 2 or 3-dimensional models, particularly where the boundary conditions are concerned. This is a very important feature since, in mathematical models, one of the most difficult problems is that of boundary conditions. The monitoring required for a 3-dimensional water quality model of an estuary would be almost impossible to meet, unless numerous simplification hypotheses are made which could destroy the supplementary precision given by a 3-dimensional study.

Moreover, where transverse gradients are not too large, a cross-section averaged value for BOD, DO, salinity or, in our case, temperature is usually sufficient for decision-making in view of all the other factors and unknowns which have to be taken into account. The hypothesis of a small transverse gradient is not met when stratification occurs, as in the vicinity of waste disposal devices, so that in those areas a 2 or 3-dimensional near field study adds substantial knowledge to the temperature or substance distribution. Though, in most cases, a relative cross-sectional homogeneity is rapidly reached so that the zones where the results of a 1-dimensional model lack precision are very restricted.

Further justification for developing 1-dimensional models for water quality lies in the fact that their range of application covers a substantial part of the waste disposal sites.

With the preceding remarks in mind, the most general form of the 1-dimensional heat transfer equation for a variable area river or estuary is as follows:

$$\frac{\partial}{\partial t}(A\rho cT) + \frac{\partial}{\partial x}(Q\rho cT) = \frac{\partial}{\partial x}\left[AE_L \frac{\partial}{\partial x}(\rho cT)\right] + \phi_n b + WHD + THD \quad (2\text{-}1)$$

where

A = cross-sectional area of river or estuary (ft^2)

T = cross-section averaged water temperature (°F)

Q = discharge (cfs) of the river or estuary (including tidal flow)

E_L = longitudinal dispersion coefficient (ft^2/sec)

ϕ_n = net heat flux into water surface (BTU/ft^2.sec)

b = top width of river or estuary (ft)

x = longitudinal distance along the axis of the river or estuary (ft)

t = time (sec.)

ρc = (density) (specific heat) = 62.4 BTU/ft^3.°F

WHD = waste heat discharge term (BTU/ft.sec)

THD = tributary heat discharge term (BTU/ft.sec)

The tributaries and waste heat discharges are considered as point injections. The corresponding terms in Equation 2-1 are:

$$WHD = \sum_i H_i \, \delta(x - x_i) \quad (2\text{-}1a)$$

where

H_i = heat discharge at injection point i (BTU/sec.)

x_i = abscissa of injection point i (ft)

δ = Dirac delta function (dimension 1/length)

and

$$THD = \sum_j Q_j \rho c T_j \, \delta(x - x_j) \quad (2\text{-}1b)$$

Where,

Q_j = discharge of triburary j. (cfs)

T_j = water temperature of tributary j. (°F)

x_j = abscissa of tributary j. (ft)

2.2 Net Surface Heat Flux: ϕ_n

Heat transfer between a body of water and the environment can occur through the free surface and through the bottom and sides. In the latter case, the heat flux is limited by conduction in the adjacent soil and remains very small because of the generally low thermal conductivity of earth and because the temperature gradients are limited. Across the water surface heat transfer by radiation, convection and evaporation is several orders of magnitude higher and only these terms will be considered here. Figure 2-1, taken from reference 2, shows schematically the more important phenomena which contribute to the surface heat transfer. Not considered here are the fluxes due to the heat contained in the evaporated water and in the direct rainfall. Those terms are usually of much smaller magnitude and can be neglected. Though, the argument that they tend to cancel each other is not fully valid, since evaporation and precipitation do not generally occur together and cancelation only happens in long-term averages.

Estimation of those various components has been the subject of many theoretical and field studies and most of the derived equations are semi-empirical. The following development is largely taken from reference 2, where the current formulae are commented upon and new contributions have been made to the determination of the heat flux in the case of an

artificially heated water surface.

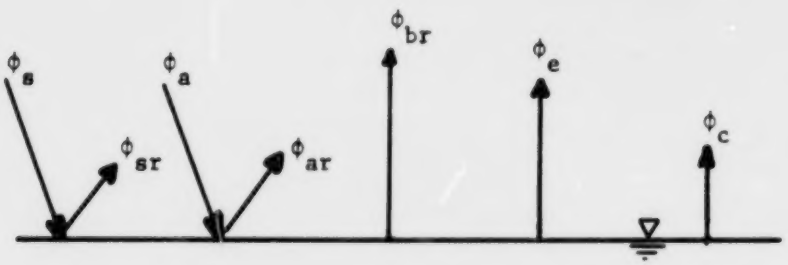

Figure 2-1. Heat Transfer Mechanisms at the Water Surface.

in which (units - energy/area.time)

ϕ_s = incident solar radiation (short wave)

ϕ_{sr} = reflected solar radiation

ϕ_{sn} = net incident solar radiation = $\phi_s - \phi_{sr}$

ϕ_a = incident atmospheric radiation (long wave)

ϕ_{ar} = reflected atmospheric radiation

ϕ_{an} = net incident atmospheric radiation = $\phi_a - \phi_{ar}$

ϕ_{br} = long wave radiation from the water surface

ϕ_e = evaporative heat flux

ϕ_c = conduction (sensible) heat flux

The units used in the following equations and formulae will be stated as often as possible; they correspond to those currently used in meteorology in the U.S., with all their incoherence. Fluxes will be measured in BTU/ft^2.-day, temperatures in °F, pressures in millimeters of mercury (mm. Hg), wind speeds in miles per hour (mph.) and heights in meters.

2.2.1 Short Wave Solar Radiation: ϕ_{sn}

Incident Radiation: ϕ_s. The short wave solar radiation received by the earth undergoes a number of complex processes as it goes through the atmosphere. Interaction with gases, water vapor, clouds and dust particles cause reflection, scattering and absorption of the solar energy which is difficult to account for with precision using only the laws of physics or empirical formulae. If an accurate value is required, direct measurement is the only reliable method. Though, numerous formulae and procedures have been given to compute the incident solar energy, from the use of empirical curves to detailed consideration of physical laws. Such methods are out of the scope of this study and are described in other works, (references 2 and 3).

Reflected Radiation: ϕ_{sr}. Various empirical formulae are available to account for the phenomena. Since it only represents 5 to 10% of the incident solar energy, a very precise determination is not necessary and Table 2-1, derived from Lake Hefner study and taken from (2), is thought to be sufficient in most cases.

Table 2-1. Ratio of reflected to incident solar radiation

Month	Jan	Feb	Mar	Apr	May	June	July	Aug	Sept	Oct	Nov	Dec
ϕ_{sr}/ϕ_s(%)	9	7	7	6	6	6	6	6	7	7	9	10

2.2.2 Longwave Atmospheric Radiation

Incident Radiation: ϕ_a. The atmosphere is a major source of radiated energy. Since its temperature is very low compared to that of the sun, the radiations are at much longer wave lengths (1 - 25μ). The

primary radiating elements are water vapor, carbon dioxide and ozone. Since the emission spectrum of the atmosphere as a whole is highly irregular, the radiated flux can only be computed through empirical relationships. Those usually deal with the atmospheric emissivity E_a which can be considered as an average emittance over the emission spectrum:

$$E_a = \frac{\phi_a}{\sigma(T_a + 460)^4} \qquad (2\text{-}2)$$

where

ϕ_a = atmospheric radiation flux

σ = Stephan Bolzman constant = $0.1713\ 10^{-8}$ BTU/ft^{-2} hr^{-1} °F^{-4}

T_a = atmospheric temperature (°F)

The influence of the clouds is usually accounted for separately, so that the above formula is valid for clear sky radiation ϕ_{ac}. Various shapes have been given to E_{ac}. Some formulae only include the vapor pressure as the one derived by Anderson (1954) from the Lake Hefner studies:

$$E_{ac} = 0.740 + 0.0065\ e_a \qquad (2\text{-}3)$$

where

e_a = atmospheric vapor pressure (mm. Hg)

Swinbank (1963) and Idso and Jackson (1969) have proposed formulae where E_{ac} is only a function of T_a. Stated directly in terms of radiation, Swinbanks' formula is:

$$\phi_{ac} = 1.2\ 10^{-13}\ (T_a + 460)^6 \qquad (2\text{-}4)$$

and Idso and Jackson's is:

$$\phi_{ac} = 4.15\ 10^{-8}\ (T_a + 460)^4\ [1 - .261\ \exp(-2.4\ 10^{-4}\ (T_a-32)^2]\quad (2\text{-}5)$$

where

T_a = air temperature at 2 m in °F

ϕ_{ac} = clear sky atmospheric radiation (BTU/ft^2-day)

Those two relationships give very similar values for temperatures higher than 50°F but the last one gives better results below 40°F. Though, Swinbank's formula was used in this study as the atmospheric temperatures rarely went below 40°F.

Clouds tend to blacken the atmosphere thus increasing the radiation. Their effects are accounted for by a formula of the type

$$\phi_a = \phi_{ac}\ (1+kC^2) \qquad (2\text{-}6)$$

where

k = constant depending on the type, thickness and height of the clouds

C = cloudiness ratio (0 for clear sky to 1 for overcast)

an average value of 0.17 is suggested for k.

Reflected Radiation: ϕ_{ar}. A figure of 3% is usually accepted as reflectance (or albedo) for a water surface to longwave radiations.

$$\phi_{ar} = 0.03\ \phi_a \qquad (2\text{-}7)$$

Net Radiation: ϕ_{an}. Putting together the preceding results gives

for the net long wave flux

$$\phi_{an} = 1.16\ 10^{-13}\ (T_a + 460)^6\ (1 + 0.17C^2) \qquad (2\text{-}8)$$

2.2.3 Longwave Radiation from the Water Surface

This term is usually the largest of all the fluxes defined in Figure 2-1. The emissivity of a water surface is known with good precision and this longwave back-radiation can be determined with accuracy inasmuch as the water surface temperature is known precisely. This is not always the case as a coll layer usually forms near the surface which is too thin to allow a temperature measurement. But the following formula gives a good enough approximation in view of all the errors introduced in the determination of the other fluxes.

$$\phi_{br} = 4.0\ 10^{-8}\ (T_s + 460)^4 \qquad (2\text{-}9)$$

where

T_s = surface temperature in °F

ϕ_{br} = back-radiation flux in BTU/ft^2.day.

2.2.4 Evaporative Flux

Evaporation from a water surface can occur as a result of both forced convection (due to the wind) and free convection (due to the buoyancy effects). At natural water surface temperatures free convection is negligible compared to forced convection. Though, when the water temperature is increased, due to heavy heat loads for instance, free convection becomes sizable and has to be accounted for.

Many different approaches have been taken to determine the evaporative mass flux from a water surface. Most of the resulting semi-

empirical formula can be written in the following form:

$$E = \rho F(W_z)\ (e_s - e_z) \qquad (2\text{-}10)$$

where

E = evaporative mass flux (mass/time.area)

ρ = density of water

W_z = wind speed at height z

$F(W_z)$ = wind speed function for mass flux including both free and forced convection effects (length/time.pressure)

e_s = saturated vapor pressure at the temperature of the water surface

e_z = vapor pressure at height z

So that the evaporative heat flux is:

$$\phi_e = L_v E \qquad (2\text{-}11)$$

where L_v is the latent heat of vaporization. Within the range of temperatures encountered in the bodies of water under study, L_v can be taken as a constant and the heat flux becomes:

$$\phi_e = f(W_z)\ (e_s - e_z) \qquad (2\text{-}12)$$

where

$f(W_z)$ = wind speed function for heat flux (energy/area.time.pressure)

Natural or Unheated Water Surface: The number of formulae available to evaluate $f(W_z)$ is great. A more detailed discussion of their value is given

in reference 2, which conclusions we shall follow here, taking a reference height of 2 m and

$$f(W_z) = 17\ W_2 \quad BTU/ft^2.day.mm\ Hg \tag{2-13}$$

where W_2 is the wind speed at 2 m in miles per hour.

And

$$\emptyset_e = f(W_2)\ (e_s - e_2) \tag{2-14}$$

Artificially Heated Water Surface. For a zero wind velocity, mass transfer by turbulent free convection can be accounted for by a diffusive type equation:

$$E = K_m \frac{\partial \rho_v}{\partial z} \tag{2-15}$$

where

E = mass flux of water vapor across the free surface

ρ_v = vapor density

K_m = vapor eddy diffusivity

z = altitude

If a simple analogy is made with turbulent free convection heat transfer (flat plate analogy) Equation 2-15 can be transformed to yield

$$\emptyset_e = 22.4\ (\Delta\theta)^{1/3}\ (e_s - e_a) \tag{2-16}$$

where

$\Delta\theta = T_s - T_a$

T_s = water surface temperature (°F)

T_a = air temperature (°F)

e_a = atmospheric vapor pressure (mm Hg)

Theoretically T_a and e_a should be measured at the same height.

Since water vapor is lighter than air, evaporation increases the buoyant driving forces. This effect is taken care of by substituting virtual temperatures for actual ones in Equation (2-16) which becomes

$$\phi_e = 22.4\ (\Delta\theta_v)^{1/3}\ (e_s - e_a) \qquad (2\text{-}17)$$

where

$$\Delta\theta_v = T_{sv} - T_{av}$$

and

$$T_{sv} = (T_s + 460)/(1 - 0.378\ e_s/p)$$

$$T_{av} = (T_a + 460)/(1 - 0.378\ e_a/p)$$

p = atmospheric pressure (mm Hg)

It would seem logical to account for forced convection as was done in the case of an unheated water surface by a factor $17\ W_2\ (e_s - e_a)$. Though, experimental work performed by Ryan and Harleman (1973) seems to prove that the predicted evaporation is too high and they advise a coefficient of 14 instead of 17. Then for the heated water surface the wind function is:

$$f(W_2) = 22.4\ (\Delta\theta_v)^{1/3} + 14\ W_2 \qquad (2\text{-}18)$$

and

$$\phi_e = f(W_2)\ (e_s - e_a)$$

It should be noted that this formula is only valid for $e_s > e_a$, that is when evaporation actually occurs. When $e_s < e_a$ there may be condensation but little is known about the heat transfer in that case and it will be set to zero in the rest of this study. Fortunately, this situation rarely happens.

In the case of a river or estuary, the limit between a heated and a natural water surface is difficult to define as the temperature continuously decreases after a waste heat discharge, finally to reach values very near the normal. Though for the purpose of computing the total surface heat flux at each point of the river or estuary, a precise transition point has to be set. Arguing that there should be no discontinuity in the evaporation rate as the surface temperature varies, this limit was set at the point where the evaporative fluxes computed with Equation 2-14 (unheated surface) and 2-18 (heated water surface) are equal; that is when

$$22.4\ (\Delta\theta_v)^{1/3} + 14\ W_2 = 17\ W_2$$

or

$$\Delta\theta_v = 0.0024\ W_2^3 \qquad (2\text{-}19)$$

When the meteorological conditions are known, this equation has to be solved by trial and error for T_s, since it also includes the saturation vapor pressure e_s which is a function of T_s. For that purpose a third degree polynomial was fitted to the tabulated values of the saturation vapor pressure in the probable range of utilization (32°F - 90°F):

$$e_s = -2.4875 + 0.2907\ T - 0.00445\ T^2 + 0.0000663\ T^3 \qquad (2\text{-}20)$$

The maximum error introduced by this approximation is 5% at 32°F and 1% at 90°F.

A plot of the evaporative heat flux versus temperature is given on Figure 2-2 which shows the position of the transition point.

2.2.5 Conduction Heat Flux $\emptyset_c$

Assuming that eddy diffusivity of heat and mass are identical, Bowen (1926) related the conduction flux to the evaporation through a ratio, now known as the Bowen ratio R.

$$R = \frac{\emptyset_c}{\emptyset_e} = .255 \left| \frac{T_s - T_z}{e_s - e_z} \right| \qquad (2\text{-}21)$$

the temperatures being expressed in °F and the vapor pressures in mm Hg. The validity of this approach has often been put into doubt, but this formula remains the most consistent with measurements.

2.2.6 Net Surface Heat Flux: $\emptyset_n$

Gathering the results of the preceding pages gives a general formula for the net surface heat flux.

$$\emptyset_n = \emptyset_s - \emptyset_{sr} + \emptyset_a - \emptyset_{ar} - \emptyset_{br} - \emptyset_e - \emptyset_c \qquad (2\text{-}22)$$

The determination of the solar and atmospheric radiation terms does not require the knowledge of the water surface temperature and the fluxes contributing to these terms will be grouped in a net radiation term $\emptyset_r$.

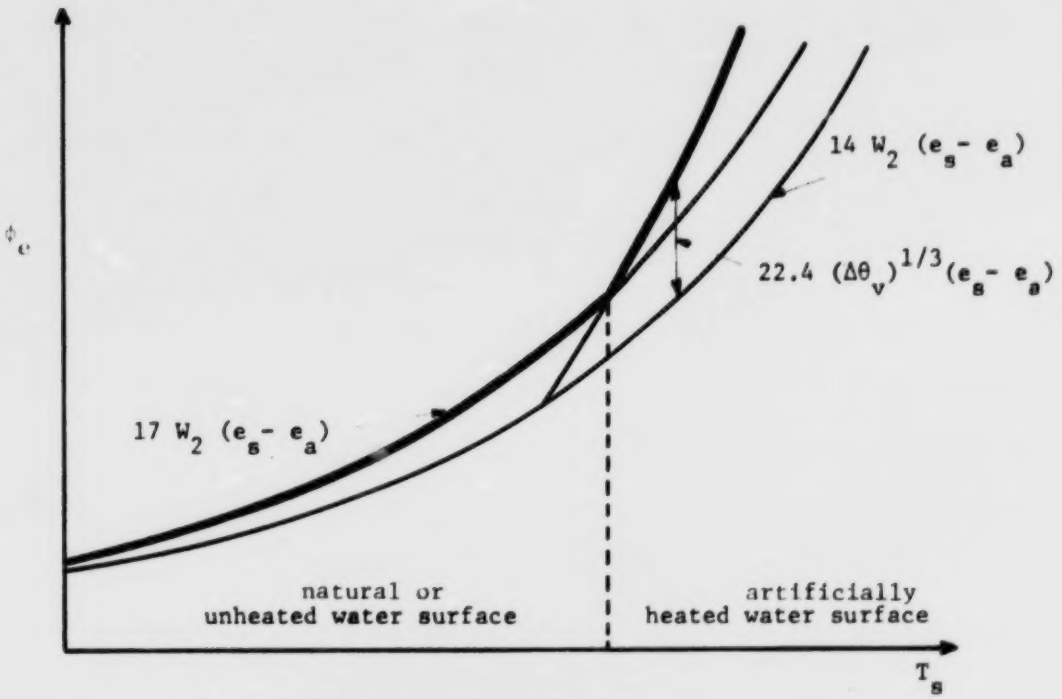

Figure 2-2. Evaporative heat flux versus surface temperature.

$$\phi_r = \phi_s - \phi_{sr} + \phi_a - \phi_{ar}$$

$$= \phi_{sn} + 1.16\ (T_a + 460)^6\ (1 + 0.17C^2) \qquad (2\text{-}23)$$

It should be noted that this net radiation term does not include the longwave radiation from the water surface.

Then an expression for the net surface heat flux is:

$$\phi_n = \phi_r - \{4\ 10^{-8}(T_s + 460)^4 + f(W)[(e_s - e_a) + .255(T_s - T_a)]\} \qquad (2\text{-}24)$$

Following is a summary of the data requirements for the computation of the net surface heat flux. These data requirements can be divided in two categories:

- Meteorological conditions (MC) which can often be considered as constant over the length of the river or estuary under study, but which are variable with time. They are:

ϕ_r: net radiation term (BTU/ft^2.day)

T_a: ambient temperature (°F)

r: relative humidity = $e_a/e_{a\ sat}$

W_2: wind velocity at 2 m (miles per hour)

p: atmospheric pressure (mm Hg)

- Water surface temperature T_s (°F) which varies with distance as well as with time.

For further use, the net surface heat flux will be written:

$$\phi_n = \phi_n(MC, T_s)$$

2.2.7 Equilibrium Temperature Concept

The equilibrium temperature T_E is defined as the temperature at which, given a set of meteorological conditions, the net surface heat flux is equal to zero. It is a solution to the equation

$$\phi_n(MC, T_E) = 0 \qquad (2\text{-}25)$$

and so, is only dependent on the meteorological conditions.

Reference 2 gives a way to solve this equation, using several approximations, but the method still involves the assumption of a value

for T_E which is later checked and adjusted, so that it is believed here, that a direct trial and error solution of Equation 2-25 is the best way to determine T_E. It is more precise and does not introduce more complication, especially when a computer is to be used.

2.2.8 Linearization of the Net Heat Flux Equation

For a given set of meteorological conditions, the typical shape of the curve of the net surface heat flux versus temperature is shown on Figure 2-3.

Considering the errors introduced in the determination of ϕ_n, due to the utilization of empirical formulae and to the space averaging of the meteorological measurements, a linear approximation of the type

$$\phi_n \simeq - K (T_s - T_E) \qquad (2\text{-}26)$$

can be considered as sufficient, particularly when the instantaneous temperature distribution in the body of water under study does not present a large difference between the maximum and the minimum. This is usually the case in rivers and estuaries, in the natural state, but also, to a lesser extent, when they are subject to waste heat loads as the local temperature increases are now limited by law.

Though, if the approximation given Equation 2-26 is to be good, the average surface temperature has to be taken into account in the determination of K, as shown on Figure 2-3.

Here also, a method, involving a number of approximations, is described in reference 2 to determine K. This method requires the

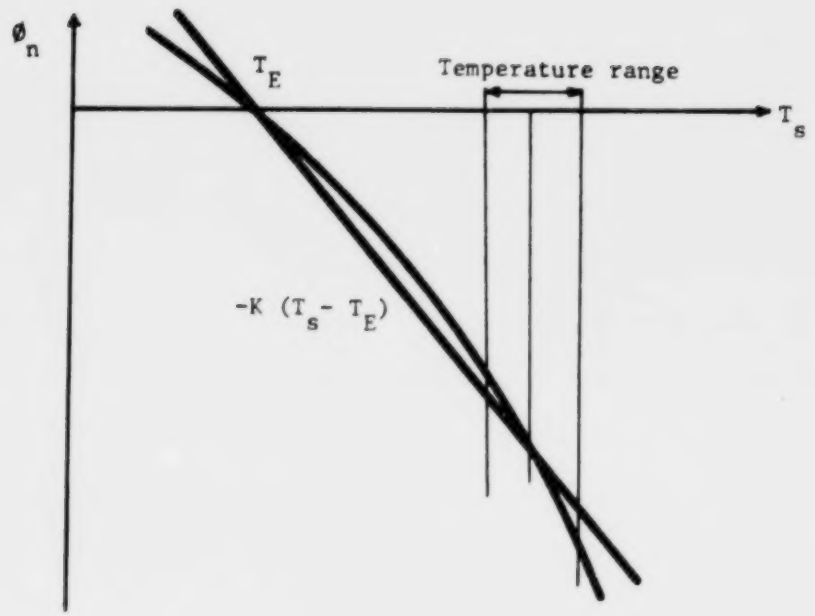

Figure 2-3. Net surface heat flux versus temperature.

knowledge of the surface temperature and of the equilibrium temperature. Since an equation already exists (Equation 2-24) to determine ϕ_n, the only interest of this linear approximation is its linearity with respect to the surface temperature, which allows an easier solving of equations involving ϕ_n. Then, once an approximation of the surface temperature is known, the easiest and most precise way to determine K is to compute ϕ_n through Equation 2-24 and let $K = -\phi_n/(T_s - T_E)$. The units for K are $BTU/ft^2.day.°F$.

2.3 Transformation of the Heat Transfer Equation

Introducing the linearized form of the surface heat flux into the general form of the heat transfer Equation (2-1) gives

$$\frac{\partial}{\partial t}(A\rho cT) + \frac{\partial}{\partial x}(Q\rho cT) = \frac{\partial}{\partial x}\left[AE_L \frac{\partial}{\partial x}(\rho cT)\right] - b\,K\,(T_s - T_E) + WHD+THD \quad (2\text{-}27)$$

If there is no vertical stratification, the surface temperature T_s is equal to the cross-section averaged temperature T. This is rarely true but, when the average velocity is large enough to ensure good mixing, the error introduced by this approximation is small. Though, one must always make sure that this approximation is valid before introducing it into Equation 2-27. If this is the case, the number of unknown functions is reduced to one in Equation 2-27 which, then, allows the determination of the temperature distribution in the river or estuary under study, provided appropriate initial and boundary conditions are furnished. It is possible to determine the temperature distribution with or without waste heat discharge from power plants by including or excluding the WHD term. Let T(t,x) be the cross-section averaged temperature at time t and abscissa x, with waste heat discharges, and $T_N(t,x)$ the normal temperature, that is without waste heat discharge, at the same time and location. Substituting in Equation 2-27 gives:

$$\frac{\partial}{\partial t}(A\rho cT) + \frac{\partial}{\partial x}(Q\rho cT) = \frac{\partial}{\partial x}\left[AE_L \frac{\partial}{\partial x}(\rho cT)\right] - b\,K(T)\,(T-T_E) + WHD+THD \quad (2\text{-}28)$$

$$\frac{\partial}{\partial t}(A\rho cT_N) + \frac{\partial}{\partial x}(Q\rho cT_N) = \frac{\partial}{\partial x}\left[AE_L \frac{\partial}{\partial x}(\rho cT_N)\right] - b\,K(T_N)\,(T_N-T_E) + THD \quad (2\text{-}29)$$

where the dependence of the temperature on K is noted by writing K = K(T). This dependence will be studied in greater detail in Chapter 3, but if T and T_N are sufficiently close at all times and locations to allow the

approximation $K(T) = K(T_N)$, Equations 2-27 and 2-28 can be subtracted to yield

$$\frac{\partial}{\partial t}(A\rho c\ \Delta T_N) + \frac{\partial}{\partial x}(Q\rho c\ \Delta T_N) = \frac{\partial}{\partial x}\left[AE_L \frac{\partial}{\partial x}(\rho c\ \Delta T_N)\right] - b\ K(T)\ \Delta T_N + WHD \quad (2\text{-}30)$$

where $\Delta T_N = T - T_N$ is the temperature excess over the normal due to the waste heat discharge. This value is interesting as it can be considered a measure of the thermal pollution.

Equation 2-30 is very similar to the BOD mass transport equation:

$$\frac{\partial}{\partial t}(AL) + \frac{\partial}{\partial x}(QL) = \frac{\partial}{\partial x}\left[AE_L \frac{\partial L}{\partial x}\right] - K_1 AL + \text{Discharges} \quad (2\text{-}31)$$

where

L = BOD concentration

K_1 = BOD decay coefficient (dimension: 1/time)

though major differences exist:

a) In the BOD case, the decay is proportional to the amount of BOD present in a control volume, which gives the term $-K_1AL$ in Equation 2-31; whereas in the temperature case, the heat loss is proportional to the free surface area of the considered body of water, which gives the term $-K\ b\ \Delta T$ in Equation 2-30.

b) In the BOD case, the decay coefficient K_1 can be considered as constant; whereas for the temperature it varies with time, since it is dependent on the meteorological conditions; and with distance, since it is dependent on the surface temperature. The dependence on the time is very important since this equation treats unsteady flows and since

the relative amplitude of the variations are large, as between day and night. For instance, in extreme tidal flow cases, where the amplitude of the tide is of the same order of magnitude as the mean water depth, the temperature difference between two low water slacks can be as high as 10°F according to the time of the day. Taking a constant K would suppress those differences which can be very significant to the aquatic life.

c) The knowledge of ΔT_N is usually insufficient when an assessment is to be made regarding the impact on the ecology and it does not allow any verification of the model since the temperature excess cannot be determined by measurement.

This shows that temperature cannot be treated exactly as BOD and the model described in Reference 1, where Equation 2-31 is solved, has to be modified to account for those differences. Equation 2-1 will be solved directly, computing ϕ_n from Equation 2-24, since the introduction of the linearized form of the surface heat flux loses much of its interest when both K and T_E are variable.

A full discussion of this approach is given in Chapter 4, but before that, a steady model will be considered which allows a better understanding of some of the phenomena involved.

III. STEADY STATE MODEL

3.1 Hypotheses

In this simplified model the hypothesis is made of a steady situation for the meteorological conditions as well as for the river discharge. A steady river discharge implies constant velocities and cross-sectional areas with time, as can be seen from the continuity and momentum equations which govern the flow. Though, the cross-sectional area is allowed to vary with distance.

3.2 Possible Applications

Although steady state conditions are never met strictly since the river discharge varies along the year, and so do the meteorological conditions, this model has the advantage of simplicity and can be applied in many cases as a first approximation by taking average conditions over a limited period of time -- a month for instance.

Moreover, this model determines the temperature and not the temperature excess as many which are derived from Equation 2-30. This allows much easier verifications and eventually adjustments over the average conditions chosen.

We saw in Chapter 2 that the heat decay coefficient varies with the surface temperature as well as with the meteorological conditions. In this steady state model, since the meteorological conditions are held constant and since the surface heat flux is computed directly from Equation 2-24, exact values of the decay coefficient can be obtained. and the influence of the surface temperature on it, can be explored

In this model, as well as in the unsteady one described in Chapter 4, the meteorological conditions are considered as constant over the

whole length of the river or estuary under study. The degree of exactitude of this approximation depends on the length considered, but, in any case, some errors are introduced. Moreover, since a continuous record of the required meteorological parameters is rarely available, time-averaged values over periods of 1 to 3 hours or more will be used in the unsteady model. Supplementary errors are introduced by this procedure. In order to obtain an idea of the subsequent errors in the temperature distribution a sensitivity analysis will be performed in which a correlation coefficient will be computed between each of the meteorological parameters and a representative characteristic of the temperature distribution.

3.3 Development of the Model

Under the assumptions stated in 3-1 the general one-dimensional heat transfer equation

$$\frac{\partial}{\partial t}(A\rho cT) + \frac{\partial}{\partial x}(Q\rho cT) = \frac{\partial}{\partial x}\left[AE_L \frac{\partial}{\partial x}(\rho cT)\right] + b\,\phi_n \qquad (3\text{-}1)$$

becomes, for steady state conditions,

$$\frac{\partial}{\partial x}(Q\rho cT) = \frac{\partial}{\partial x}\left[AE_L \frac{\partial}{\partial x}(\rho cT)\right] + b\,\phi_n \qquad (3\text{-}2)$$

For a river, the dispersive term can be neglected and in a zone where there is no tributary, $\partial Q/\partial x = 0$. Within the range of variation of the temperature the term ρc can be assumed to be constant and the final form of the equation is:

$$\frac{dT}{dx} = \frac{\phi_n(T)\, b(x)}{\rho cQ} \qquad (3\text{-}4)$$

This first order ordinary differential equation can be solved if one boundary condition is prescribed. The easiest way to do it, both in the field and for the model, is to specify the temperature at the upstream end of the river portion under study.

$$T = T_o \quad \text{at} \quad x = x_o \tag{3-5}$$

Discontinuities appear if there are tributaries or waste heat discharges. At those points dT/dx is no longer defined and there is a change in the discharge Q so that Equation 3-5 is not valid and a new upstream boundary condition should be specified.

If at $x = x_A$ there is a tributary with a discharge Q_A and an average temperature T_A the new discharge will be $Q + Q_A$ and the new upstream boundary condition

$$T = \frac{QT(x_A) + Q_A T_A}{Q + Q_A} \quad \text{at} \quad x = x_A \tag{3-6a}$$

If the discontinuity is due to a waste heat input of H BTU/sec., there will be no change in the discharge since the inplant water losses are usually small compared to the river discharge and the new upstream boundary condition will be:

$$T = T(x_A) + \frac{H}{\rho c Q} \quad \text{at} \quad x = x_A \tag{3-6b}$$

Simplified Case

If the width b is constant and if the surface heat loss coefficient K is assumed to be independent of the river temperature, that is, if we take

$$\phi_n = -K\ (T - T_E) \tag{3-7}$$

Equation 3-4 becomes

$$\frac{dT}{dx} = -\frac{K\ b}{\rho c Q}\ (T - T_E) \tag{3-8}$$

and an analytical solution is easily found to be

$$T = T_E + (T_o - T_E)\ e^{-\frac{b\ K}{\rho c Q}\ x} \tag{3-9}$$

General Case (varying width)

In the general case a finite difference scheme was used to solve Equation 3-4. For that purpose a one-dimensional partition of the river is done:

$$\{x_o,\ x_1,\ x_2,\ \ldots\ ,\ x_i,\ x_{i+1},\ \ldots\ ,\ x_n\}$$

with segments $[x_i,\ x_{i+1}]$ of non-necessarily constant length to allow a smaller mesh spacing in the zones where the temperature gradients are larger.

If T_i is the cross-section averaged temperature at abscissa x_i, we have according to the Taylor formula

$$T_{i+1} = T_i + (x_{i+1} - x_i)\ \left.\frac{dT}{dx}\right|_{\xi_i} \qquad x_i \leq \xi_i \leq x_{i+1} \tag{3-10}$$

substituting in Equation 3-4 gives

$$\frac{T_{i+1} - T_i}{x_{i+1} - x_i} = \frac{\phi_n[T(\xi_i)]\ b(\xi_i)}{\rho c Q} \tag{3-11}$$

Since the temperature distribution usually has an exponential shape, ξ_i is more in the middle of the segment $[x_i, x_{i+1}]$ than at one extremity, as shown on Figure 3-1. So, the value of the width will be taken at

$$\frac{x_i + x_{i+1}}{2}$$

and, in order to simplify the geometrical data input, a linear interpolation will be performed between x_i and x_{i+1},

$$b\left(\frac{x_i + x_{i+1}}{2}\right) \simeq \frac{b(x_i) + b(x_{i+1})}{2} \qquad (3\text{-}12)$$

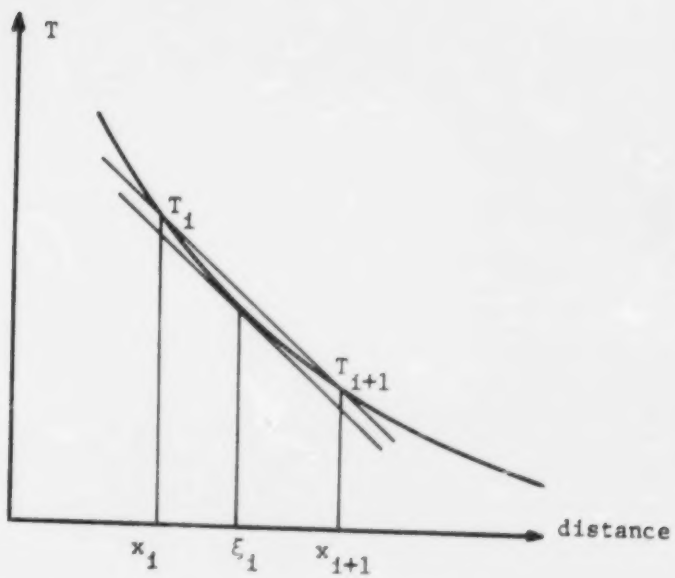

Figure 3-1. Position of ξ_i in the interval $[x_i, x_{i+1}]$.

Such a procedure cannot be applied for $\phi_n[T(\xi_i)]$ since the temperature at x_{i+1} is unknown and the functional relationship between ϕ_n and T prevents an implicit determination. So ϕ_n will be approximated at the preceding mesh point x_i. It is important to determine if such an approximation will not engender cascade errors as the numerical computations propagate. Let us consider the simplified case of a constant width. The computed temperature at abscissa x_i being $\bar{T}_i$ and the real one T_i we have:

$$\bar{T}_1 = T_o + (x_1 - x_o) \frac{\phi_n(T_o)\, b}{\rho c Q}$$

$$\bar{T}_2 = \bar{T}_1 + (x_2 - x_1) \frac{\phi_n(\bar{T}_1)\, b}{\rho c Q} \qquad (3\text{-}13)$$

$$\bar{T}_i = \bar{T}_{i-1} + (x_i - x_{i-1}) \frac{\phi_n(\bar{T}_{i-1})\, b}{\rho c Q}$$

summing up gives

$$\bar{T}_i = T_o + \frac{b}{\rho c Q}\left[(x_1 - x_o)\,\phi_n(T_o) + (x_2 - x_1)\,\phi_n(\bar{T}_1) + \ldots + (x_i - x_{i-1})\phi_n(\bar{T}_{i-1})\right] \qquad (3\text{-}14)$$

writing similar equations for the exact temperature would give

$$T_i = T_o + \frac{b}{\rho c Q}\left[(x_1 - x_o)\,\phi_n\,[T(\xi_o)] + \ldots + (x_i - x_{i-1})\,\phi_n[T(\xi_{i-1})]\right] \qquad (3\text{-}15)$$

so that

$$\bar{T}_i - T_i = \frac{b}{\rho c Q} \sum_{k=0}^{i-1} (x_{k+1} - x_k)\left[\phi_n[\bar{T}_k] - \phi_n[T(\xi_k)]\right] \qquad (3\text{-}16)$$

Let us suppose that from k = 0 to i, $\bar{T}_k - T_k$ has a constant sign. If to begin with, $T_o > T_E$, T(x) will be a decreasing function and

$$T_o > T(\xi_o)$$

since $\phi_n(T)$ is a decreasing function

$$\phi_n(T_o) < \phi_n[T(\xi_o)]$$

and

$$\bar{T}_1 - T_1 = \frac{b}{\rho c Q} (x_1 - x_o) \left[\phi_n(T_o) - \phi_n[T(\xi_o)]\right] < 0 \quad (3\text{-}17)$$

Figure 3-2 shows how the solution is approximated in this case, when $\bar{T} - T$ keeps negative.

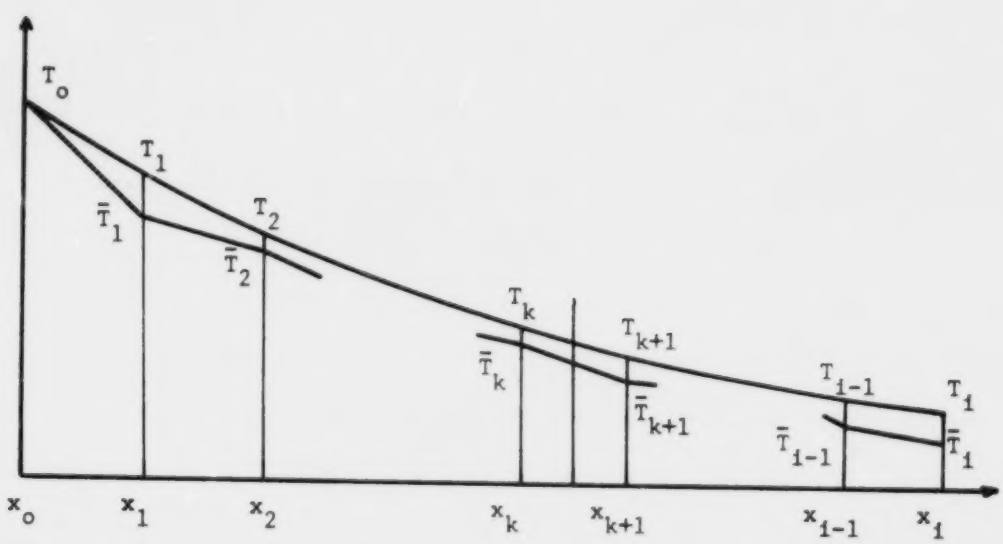

Figure 3-2. Approximation of the solution in the most unfavorable case

Then

$$\bar{T}_k < T_k \longrightarrow \quad \phi_n(\bar{T}_k) > \phi_n(T_k)$$

$$T(\xi_k) > T_{k+1} \longrightarrow \quad \phi_n[T(\xi_k)] < \phi_n(T_{k+1})$$

---

and by addition $\quad \phi_n(\bar{T}_k) - \phi_n[T(\xi_k)] > \phi_n(T_k) - \phi_n(T_{k+1})$

substituting in Equation 3-16 gives

$$\bar{T}_i - T_i > \frac{b}{\rho c Q} \sum_{k=0}^{i-1} (x_{k+1} - x_k)\left[\phi_n[T_k] - \phi_n[T_{k-1}]\right] \qquad (3\text{-}18)$$

if the mesh spacing is constant and equal to Δx

$$\bar{T}_i - T_i > \frac{b}{\rho c Q} \Delta x \left[\phi_n[T_o] - \phi_n[T_i]\right] \qquad (3\text{-}19)$$

and since $\bar{T}_i - T_i < 0$

$$\left|\bar{T}_i - T_i\right| < \frac{b\Delta x}{\rho c Q} \left[\phi_n[T_i] - \phi_n[T_o]\right] \qquad (3\text{-}20)$$

which shows that the error can be made as small as desired provided a correct value is given for Δx.

If at one point x_e, $\bar{T} - T$ changes sign, the same reasoning can be applied between this point (where $\bar{T}_e - T_e = 0$) and x_i provided the segment $[x_e, x_i]$ does not contain any more sign change. Then T_o is simply replaced by T_e in Equation 3-20. A similar development can be made for $\bar{T} - T > 0$ so that the largest bound for the error is obtained when $\bar{T} - T$ never changes sign and for T_i and T_n in Equation 3-20.

Sample Run. A run was made for the simplified case of a constant width in order to check with the analytical solution given by Equation 3-9 and to determine the influence of the surface temperature on the decay

coefficient K. Exact values of K were determined at each step by dividing the net surface flux computed with Equation 2-24 by $(T - T_E)$. T_E is determined at the beginning of each run for the corresponding meteorological conditions by trial and error. This influence of the temperature on K is particularly important in the derivation of Equation 2-29 where K is taken to be the same with and without waste heat discharge. This was explored by introducing a 400,000 BTU/sec heat input at x = 0, which gives a typical temperature excess over the normal of 6.5°F at the injection point, with the 1000 cfs river discharge chosen.

The geometrical and meteorological data for the sample run is printed at the beginning of the results outputs given in Tables 3-1 and 3-2. The resulting temperature distributions, with and without waste heat discharge are shown on Figure 3-3.

A 50 ft. mesh spacing was chosen (although the results are given every 500 ft.) so that, with the waste discharge, where the temperature variation is the largest, and so the error, the maximum error for the 47,000 ft. under study is less than

$$\frac{b\Delta x}{\rho c Q}\left[\emptyset_n\,(55.48) - \emptyset_n(61.41)\right] = 0.008$$

as given by Equation 3-20. Working with the program has shown that the error is usually much smaller (up to 5 times) but this formula has the interest of giving an upper limit which is a measure of the model precision and can be used as a discretization criteria when a value of the maximum temperature variation can be estimated beforehand.

It appears from the runs (see following pages) that the surface

TEMPERATURE DISTRIBUTION STUDY
****

BY DIRECT CALCULATION OF THE SURFACE HEAT FLUX

THE AMBIANT TEMPERATURE IS 60 DEG F
THE RELATIVE HUMIDITY IS .75
THE WIND VELOCITY AT 2 M IS 10 MI/HOUR
THE NET RADIATED FLUX IS 2500 BTU/FT2/DAY
THE ATMOSPHERIC PRESSURE IS 760 MM HG

EQUILIBRIUM TEMPERATURE 58.7969 DEG. F

THE RIVER DISCHARGE IS 1000 CFS
THE HEAT DISCHARGE IS 0 BTU/S
THE INITIAL TEMPERATURE OF THE RIVER IS 55 DEG F

STATION (ft)	WIDTH (ft)	TEMPERATURE (°F)	DECAY (BTU/°F.s.ft^2)
-0	1000	55	
+0	1000	55	
500	1000	54.9734	1.51948E-03
1000	1000	54.947	1.51914E-03
1500	1000	54.921	1.51879E-03
2000	1000	54.8954	1.51845E-03
2500	1000	54.87	1.51811E-03
3000	1000	54.845	1.51776E-03
3500	1000	54.8202	1.51745E-03
4000	1000	54.7958	1.51711E-03
4500	1000	54.7717	1.51678E-03
5000	1000	54.7478	1.51648E-03
5500	1000	54.7243	1.51616E-03
6000	1000	54.701	1.51585E-03
6500	1000	54.6781	1.51553E-03
7000	1000	54.6554	1.51524E-03
7500	1000	54.633	1.51493E-03
8000	1000	54.6108	1.51465E-03
8500	1000	54.589	1.51436E-03
9000	1000	54.5674	1.51406E-03
9500	1000	54.546	1.51377E-03
10000	1000	54.525	1.51351E-03
10500	1000	54.5041	1.51322E-03
11000	1000	54.4836	1.51293E-03
11500	1000	54.4633	1.51268E-03
12000	1000	54.4432	1.51240E-03
12500	1000	54.4234	1.51214E-03
13000	1000	54.4038	1.51187E-03
13500	1000	54.3845	1.51161E-03
14000	1000	54.3654	1.51137E-03
14500	1000	54.3465	1.51111E-03
15000	1000	54.3279	1.51086E-03
15500	1000	54.3095	1.51061E-03
16000	1000	54.2913	1.51037E-03
16500	1000	54.2733	1.51014E-03
17000	1000	54.2556	1.50990E-03
17500	1000	54.238	1.50965E-03
18000	1000	54.2207	1.50942E-03

Table 3-1. Reproduction of the computer output for the steady model sample run without heat discharge.

STATION (ft)	WIDTH (ft)	TEMPERATURE (°F)	DECAY (BTU/°F.s.ft^2)
18500	1000	54.0036	1.50920E-03
19000	1000	54.1867	1.50896E-03
19500	1000	54.17	1.50874E-03
20000	1000	54.1535	1.50853E-03
20500	1000	54.1377	1.50830E-03
21000	1000	54.1211	1.50809E-03
21500	1000	54.1052	1.50788E-03
22000	1000	54.0895	1.50767E-03
22500	1000	54.074	1.50746E-03
23000	1000	54.0587	1.50727E-03
23500	1000	54.0436	1.50704E-03
24000	1000	54.0286	1.50686E-03
24500	1000	54.0138	1.50667E-03
25000	1000	53.9993	1.50646E-03
25500	1000	53.9848	1.50629E-03
26000	1000	53.9706	1.50609E-03
26500	1000	53.9565	1.50587E-03
27000	1000	53.9426	1.50569E-03
27500	1000	53.9289	1.50553E-03
28000	1000	53.9153	1.50532E-03
28500	1000	53.9019	1.50516E-03
29000	1000	53.8887	1.50498E-03
29500	1000	53.8756	1.50480E-03
30000	1000	53.8627	1.50463E-03
30500	1000	53.8499	1.50445E-03
31000	1000	53.8373	1.50428E-03
31500	1000	53.8249	1.50409E-03
32000	1000	53.8126	1.50393E-03
32500	1000	53.8004	1.50377E-03
33000.	1000	53.7884	1.50360E-03
33500.	1000	53.7765	1.50345E-03
34000.	1000	53.7648	1.50329E-03
34500.	1000	53.7532	1.50313E-03
35000.	1000	53.7418	1.50298E-03
35500.	1000	53.7305	1.50281E-03
36000.	1000	53.7193	1.50269E-03
36500.	1000	53.7083	1.50252E-03
37000.	1000	53.6974	1.50237E-03
37500.	1000	53.6866	1.50221E-03
38000.	1000	53.676	1.50208E-03
38500.	1000	53.6654	1.50193E-03
39000.	1000	53.6551	1.50179E-03
39500.	1000	53.6448	1.50167E-03
40000.	1000	53.6347	1.50149E-03
40500.	1000	53.6246	1.50136E-03
41000.	1000	53.6148	1.50122E-03
41500.	1000	53.605	1.50108E-03
42000.	1000	53.5953	1.50096E-03
42500.	1000	53.5858	1.50083E-03
43000.	1000	53.5764	1.50068E-03
43500.	1000	53.5671	1.50056E-03
44000.	1000	53.5579	1.50046E-03
44500.	1000	53.5488	1.50030E-03
45000.	1000	53.5398	1.50017E-03
45500.	1000	53.5309	1.50007E-03
46000.	1000	53.5222	1.49994E-03
46500.	1000	53.5135	1.49983E-03
47000.	1000	53.5049	1.49973E-03

TEMPERATURE DISTRIBUTION STUDY
****

BY DIRECT CALCULATION OF THE SURFACE HEAT FLUX

THE AMBIANT TEMPERATURE IS 60 DEG F
THE RELATIVE HUMIDITY IS .75
THE WIND VELOCITY AT 2 M IS 10 MI/HOUR
THE NET RADIATED FLUX IS 2500 BTU/FT2/DAY
THE ATMOSPHERIC PRESSURE IS 760 MM HG

EQUILIBRIUM TEMPERATURE 52.7969 DEG. F

THE RIVER DISCHARGE IS 1000 CFS
THE HEAT DISCHARGE IS 400000. BTU/S
THE INITIAL TEMPERATURE OF THE RIVER IS 55 DEG F

STATION (ft)	WIDTH (ft)	TEMPERATURE(°F)	DECAY(BTU/°F.s.ft^2)
-0	1000	55	
+0	1000	61.4103	
500	1000	61.2999	1.60768E-03
1000	1000	61.1914	1.60299E-03
1500	1000	61.0845	1.59830E-03
2000	1000	60.9792	1.59361E-03
2500	1000	60.8756	1.58892E-03
3000	1000	60.7737	1.58421E-03
3500	1000	60.6733	1.57947E-03
4000	1000	60.5745	1.57470E-03
4500	1000	60.4772	1.56991E-03
5000	1000	60.3814	1.56505E-03
5500	1000	60.2871	1.56013E-03
6000	1000	60.1943	1.55512E-03
6500	1000	60.1029	1.54999E-03
7000	1000	60.0129	1.54474E-03
7500	1000	59.9244	1.53931E-03
8000	1000	59.8372	1.53366E-03
8500	1000	59.7515	1.52772E-03
9000	1000	59.6671	1.52140E-03
9500	1000	59.5841	1.51454E-03
10000	1000	59.5025	1.50690E-03
10500	1000	59.4224	1.49803E-03
11000	1000	59.3436	1.48691E-03
11500	1000	59.2666	1.46970E-03
12000	1000	59.1884	1.57792E-03
12500	1000	59.1082	1.57676E-03
13000	1000	59.029	1.57563E-03
13500	1000	58.9509	1.57451E-03
14000	1000	58.8738	1.57341E-03
14500	1000	58.7978	1.57232E-03
15000	1000	58.7227	1.57125E-03
15500	1000	58.6486	1.57019E-03
16000	1000	58.5756	1.56915E-03
16500	1000	58.5034	1.56813E-03
17000	1000	58.4322	1.56712E-03
17500	1000	58.362	1.56612E-03
18000	1000	58.2926	1.56514E-03

Table 3-2. Reproduction of the computer output for the steady model sample run with heat discharge at x = 0. (44)

STATION (ft)	WIDTH (ft)	TEMPERATURE (°F)	DECAY (BTU/°F.s.ft^2)
18500	1000	58.2242	1.56417E-03
19000	1000	58.1566	1.56321E-03
19500	1000	58.09	1.56227E-03
20000	1000	58.0242	1.56134E-03
20500	1000	57.9593	1.56043E-03
21000	1000	57.8952	1.55953E-03
21500	1000	57.8319	1.55864E-03
22000	1000	57.7695	1.55777E-03
22500	1000	57.7079	1.55690E-03
23000	1000	57.647	1.55605E-03
23500	1000	57.587	1.55521E-03
24000	1000	57.5278	1.55438E-03
24500	1000	57.4693	1.55356E-03
25000	1000	57.4116	1.55276E-03
25500	1000	57.3545	1.55197E-03
26000	1000	57.2983	1.55119E-03
26500	1000	57.2427	1.55041E-03
27000	1000	57.1879	1.54965E-03
27500	1000	57.1337	1.54890E-03
28000	1000	57.0803	1.54815E-03
28500	1000	57.0275	1.54743E-03
29000	1000	56.9754	1.54671E-03
29500	1000	56.924	1.54599E-03
30000	1000	56.8732	1.54530E-03
30500	1000	56.8231	1.54461E-03
31000	1000	56.7736	1.54392E-03
31500	1000	56.7248	1.54325E-03
32000	1000	56.6766	1.54259E-03
32500	1000	56.6289	1.54193E-03
33000.	1000	56.5819	1.54128E-03
33500.	1000	56.5355	1.54065E-03
34000.	1000	56.4897	1.54002E-03
34500.	1000	56.4444	1.53940E-03
35000.	1000	56.3998	1.53878E-03
35500.	1000	56.3556	1.53818E-03
36000.	1000	56.3121	1.53759E-03
36500.	1000	56.2691	1.53700E-03
37000.	1000	56.2266	1.53642E-03
37500.	1000	56.1847	1.53585E-03
38000.	1000	56.1433	1.53529E-03
38500.	1000	56.1024	1.53473E-03
39000.	1000	56.062	1.53418E-03
39500.	1000	56.0222	1.53363E-03
40000.	1000	55.9828	1.53310E-03
40500.	1000	55.944	1.53258E-03
41000.	1000	55.9056	1.53205E-03
41500.	1000	55.8677	1.53154E-03
42000.	1000	55.8303	1.53103E-03
42500.	1000	55.7933	1.53053E-03
43000.	1000	55.7568	1.53004E-03
43500.	1000	55.7208	1.52955E-03
44000.	1000	55.6852	1.52907E-03
44500.	1000	55.65	1.52859E-03
45000.	1000	55.6153	1.52812E-03
45500.	1000	55.5811	1.52766E-03
46000.	1000	55.5472	1.52720E-03
46500.	1000	55.5138	1.52675E-03
47000.	1000	55.4808	1.52630E-03

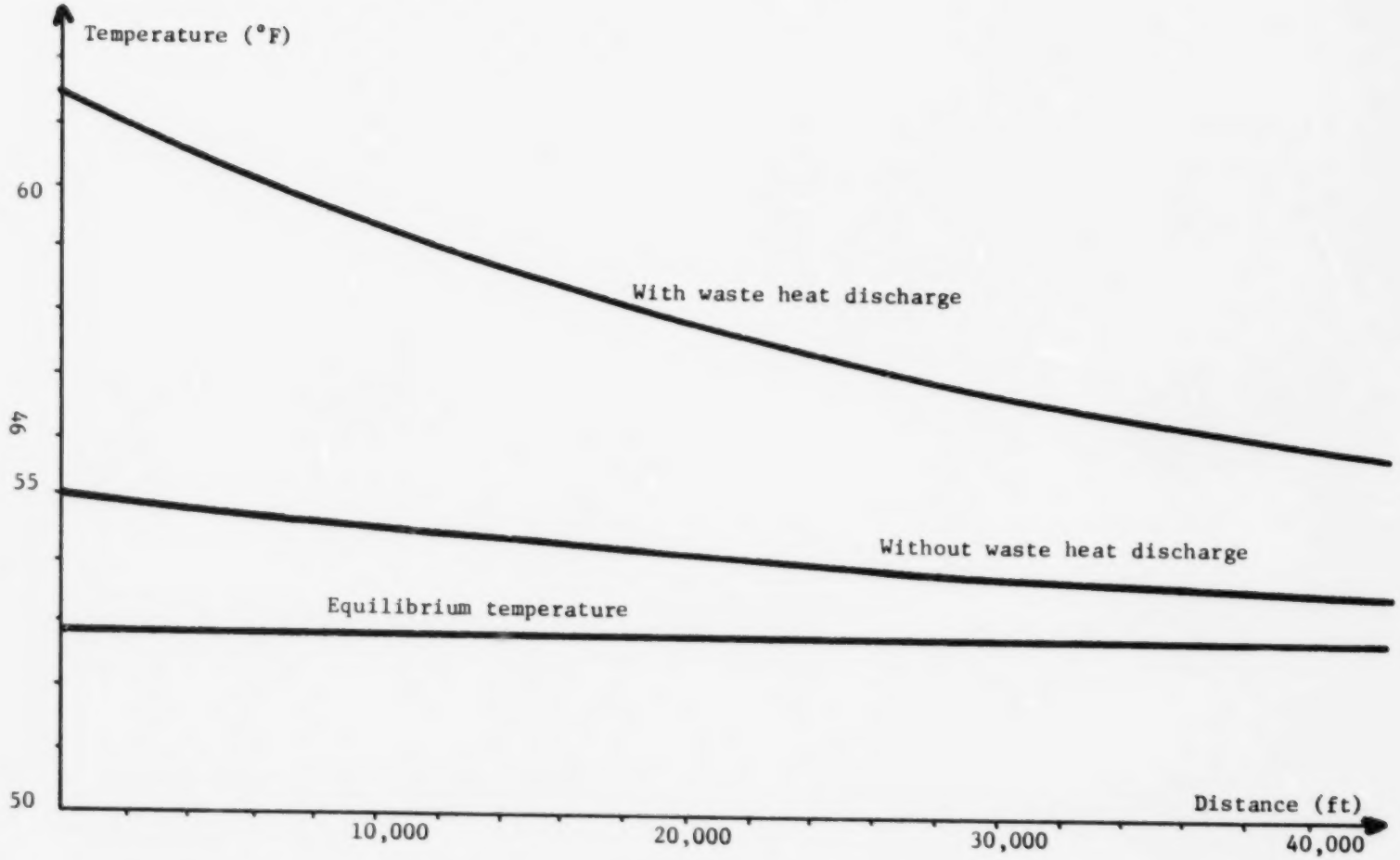

Figure 3-3. Sample run of the steady model with and without heat discharge at x = 0.

heat loss coefficient varies of about 1% per 1 degree F difference in the river temperature. So, when the temperature variation is limited, the approximation of a constant K is sufficient since the precision with which K is known can be as bad as 10% depending on the accuracy and significance of the meteorological data available.

Table 3-3 shows a comparison of the results obtained from the model and from the analytical solution for the temperature excess over the normal due to the heat discharge. The analytical solution for the temperature excess is easily derived from Equation 3-9. If K is assumed to be independent of the temperature this equation gives the normal temperature distribution as well as the temperature distribution with the heat discharge, T. Then if $\Delta T_N = T - T_N$ we obtain by subtraction

$$\Delta T_N = \Delta T_o \; e^{-\frac{b\,K}{\rho c Q}\,x} \qquad (3\text{-}21)$$

Here also it appears that if the initial temperature excess is small the approximation of a constant decay coefficient is sufficient. This is the case for most waste heat discharge disposals as environmental laws prohibit excessive local heating of streams. Though, such an approximation would be poor for cooling ponds where the intake and output temperature difference is made as high as possible.

3.4 Sensitivity Analysis

The study of the temperature distribution in free surface bodies of water requires extensive meteorological data. This data is used to determine the net surface heat flux through a semi-empirical relationship such as Equation 2-23. The mere utilization of such a formula introduces an uncertainty of about 5% in the net flux, but, added to that,

table 3-3 : COMPARISON OF THE TEMPERATURE EXCESS ($T - T_N$) WITH CONSTANT AND VARYING K

STATION (ft)	$K = 1.60 \times 10^{-3}$	$K = 1.55 \times 10^{-3}$ (BTU/°F.sec.ft^2)	$K = 1.51 \times 10^{-3}$	Varying K (Model)
0	6.41	6.41	6.41	6.41
2000	6.09	6.10	6.11	6.08
4000	5.79	5.80	5.82	5.78
6000	5.50	5.52	5.54	5.49
8000	5.22	5.26	5.28	5.23
10000	4.96	5.00	5.03	4.98
12000	4.71	4.76	4.79	4.75
14000	4.48	4.53	4.57	4.51
16000	4.25	4.31	4.35	4.28
18000	4.04	4.10	4.15	4.07
20000	3.84	3.90	3.95	3.87
22000	3.65	3.71	3.76	3.68
24000	3.46	3.53	3.59	3.50
26000	3.29	3.36	3.42	3.33
28000	3.13	3.20	3.26	3.17
30000	2.97	3.04	3.10	3.01
32000	2.82	2.90	2.96	2.86
34000	2.68	2.75	2.82	2.72
36000	2.55	2.62	2.68	2.59
38000	2.42	2.49	2.56	2.47
40000	2.30	2.37	2.44	2.35
42000	2.18	2.26	2.32	2.24
44000	2.07	2.15	2.21	2.13
46000	1.97	2.04	2.11	2.03

is a supplementary error due to the fact that the necessary meteorological parameters are not known exactly:

- The meteorological data is considered as constant over the whole length of the river or estuary under study and is often measured at only one location.

- The time varying magnitude of each of the required meteorological parameters is averaged over periods of time ranging from 1 to 3 hours or more.

- Measurements for some of the required parameters are only available from stations located a distance away from the studied body of water and the difference in surface cover (water, versus grass, forest . . .) can be of significance.

- The measurement height of some parameters (such as wind velocity) cannot always be equal to the one prescribed by some of the empirical formulae used and empirical corrections are to be performed which bring supplementary errors.

Even though it is difficult to estimate precisely the magnitude of the errors in the meteorological parameters due to the preceding facts, it is important to know what their influence can be on the subsequently computed temperature distribution. The number of parameters involved, as well as the form of the equations make it difficult to establish an error formula for the temperature distribution. So, the steady model was used to estimate the order of magnitude of those errors. For that purpose, a correlation coefficient was computed between each of the meteorological parameters and the temperature variation Δt between two

points of the river. The geometrical data used was the same as for the sample run presented before, namely, a river discharge of 1000 cfs and a top width of 1000 ft. These numbers produce a large heat decay, since the top width is large for such a discharge, so a maximum influence of the meteorological conditions is expected.

For a meteorological parameter μ the correlation coefficient is determined as follows:

$$C_{\mu} = \frac{\frac{\Delta(\Delta T)}{\Delta T}}{\frac{\Delta \mu}{\mu}} \qquad (3\text{-}22)$$

where

$\Delta T = T_x - T_0$

T_x = cross section averaged temperature at abscissa x

T_o = cross section averaged temperature at abscissa o (boundary condition)

In this case, x was chosen as 47,000 ft. which allows a large part of the temperature variation to take place.

The definition of C_{μ} is such that if a 1% error is made in the measurement of μ the corresponding error in the temperature variation is C_{μ}%.

This correlation coefficient varies with μ and with the other meteorological parameters. Figures 3-4 to 3-8 show the approximate range of variation of the correlation coefficients for relative humidity (r), net radiated flux (ϕ_r), wind velocity (W_2), ambient temperature (T_a) and atmospheric pressure (p). The two curves shown on each figure give the maximum and minimum of the correlation coefficients for other

meteorological parameters in a range plausible for an upstream temperature of 60°F.

Those curves do not allow an exact determination of the errors because of the number of parameters involved. Though, they give an order of magnitude and show that the most important parameters are the relative humidity, the net radiated flux and the ambient temperature, and that in extreme conditions the relative error in the temperature distribution can be up to 5 times the relative error in the afore mentioned parameters.

It should be pointed out that those results apply to the actual stream temperature and not to the temperature excess due to artificial heat sources. In the latter case, the surface heat loss term is $- K \Delta T_N$ (Equation 2-30) and other authors such as Jobson (4) have studied the sensitivity of this term to the various meteorological parameters. Only K is a function of the meteorological parameters and it appears that the most relevant parameters are the natural water temperature and the wind speed; the ambient temperature and relative humidity being of almost no influence. The last two parameters are of importance in the equilibrium temperature T_E which appears in the surface heat loss term $-K(T - T_E)$ governing the actual stream temperature (Equation 2-28).

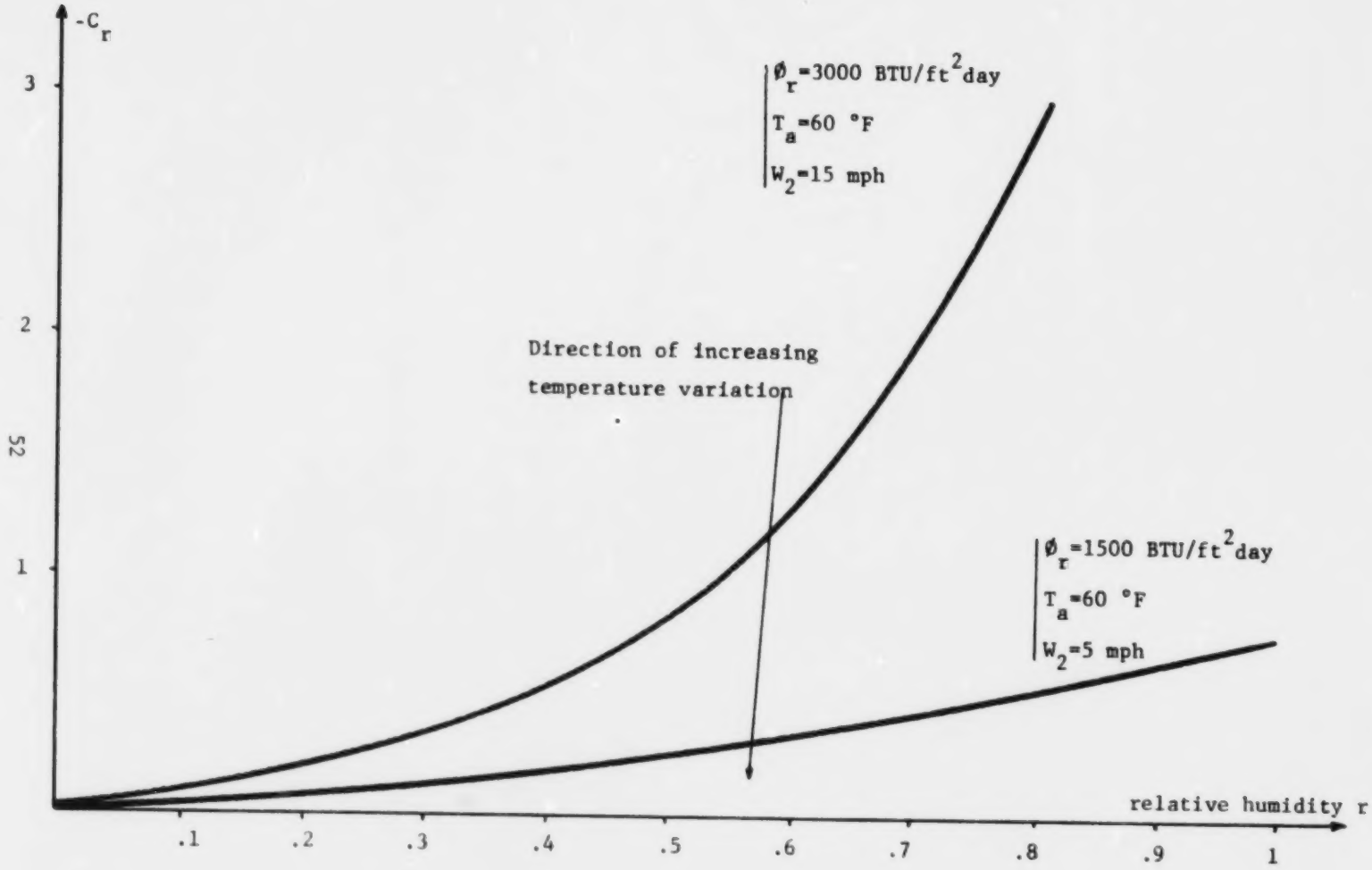

Figure 3-4. Approximate range of variation of the corrolation coefficient for relative humidity.

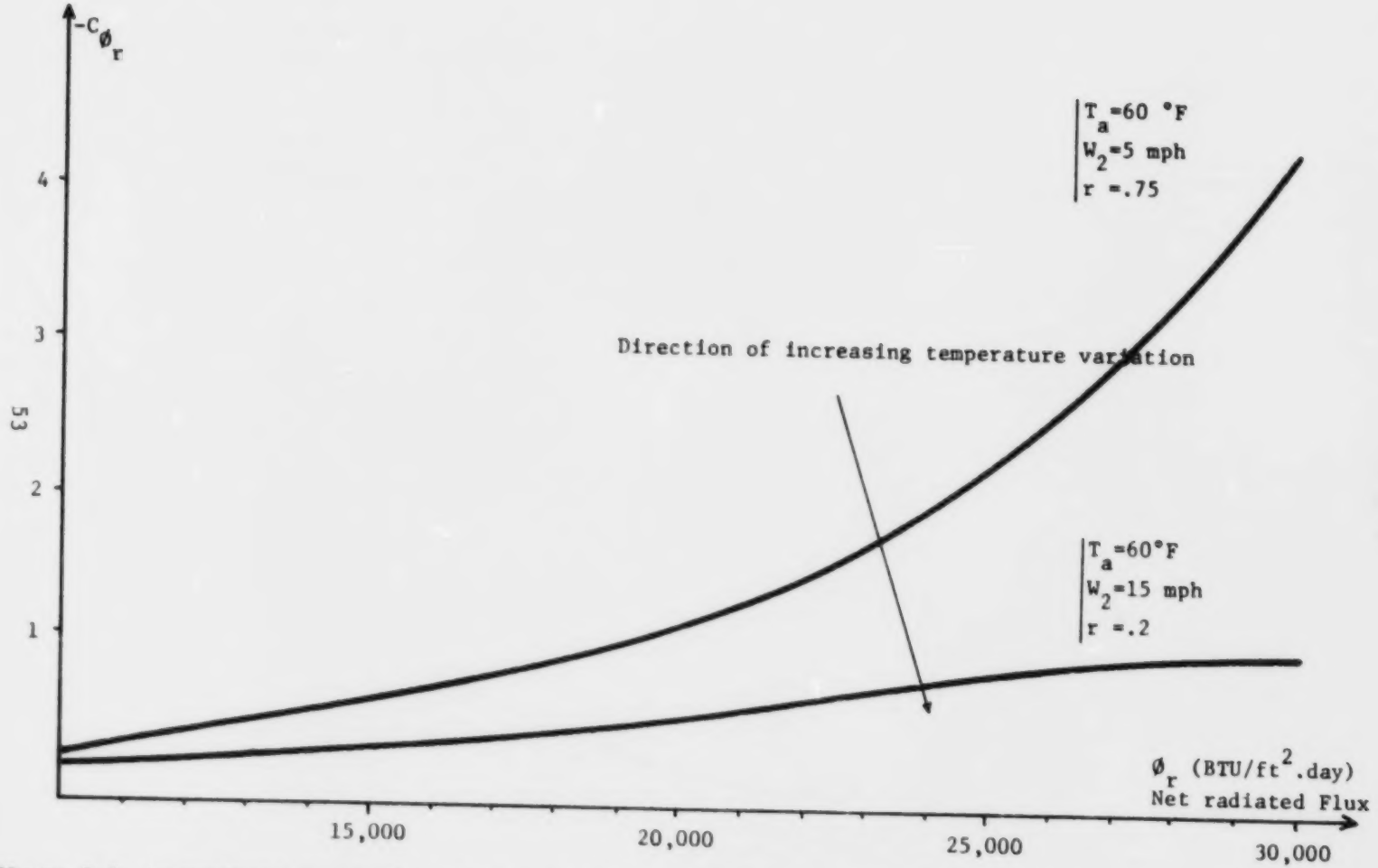

Figure 3-5. Approximate range of variation of the corrolation coefficient for the net radiated flux.

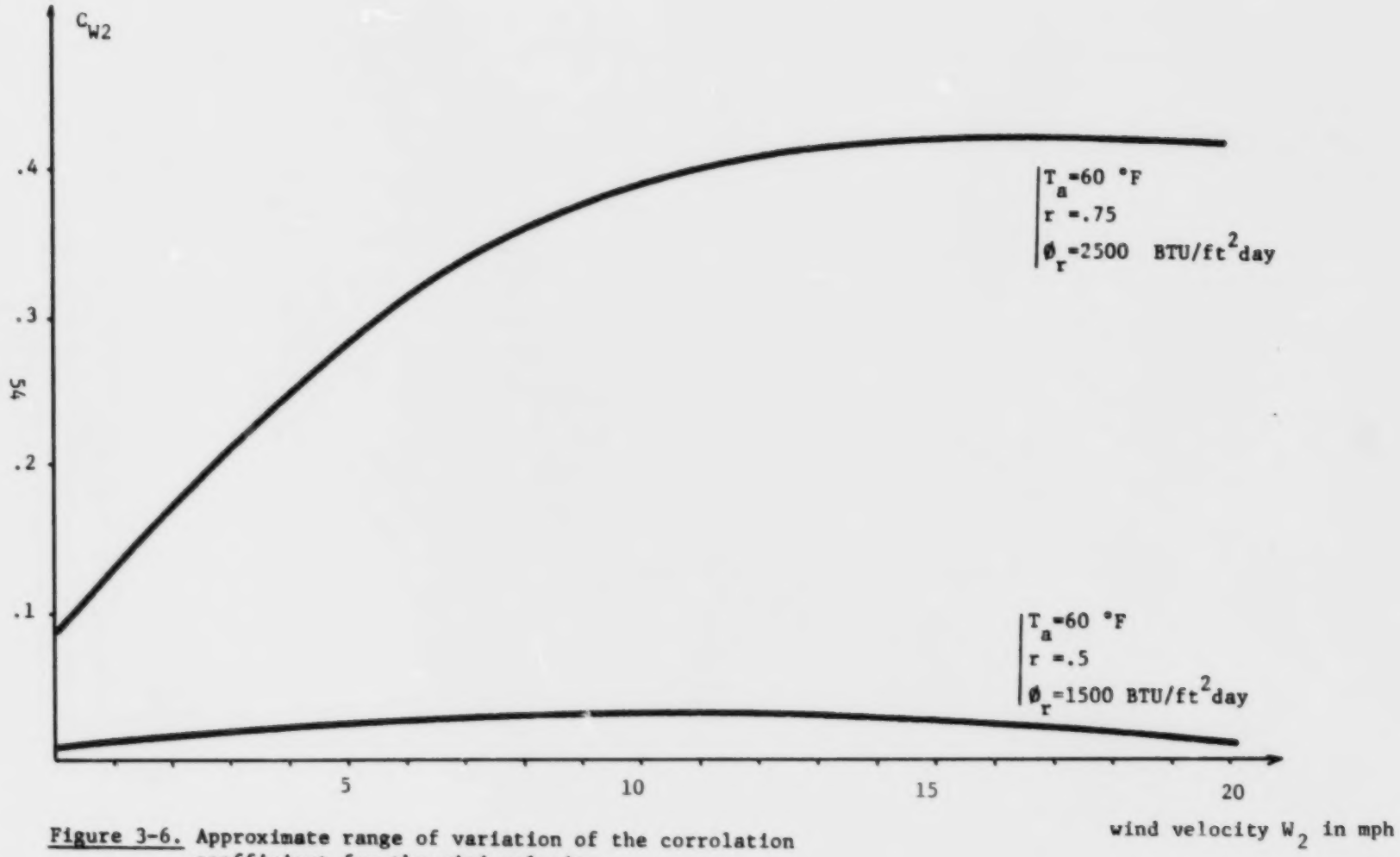

Figure 3-6. Approximate range of variation of the corrolation coefficient for the wind velocity.

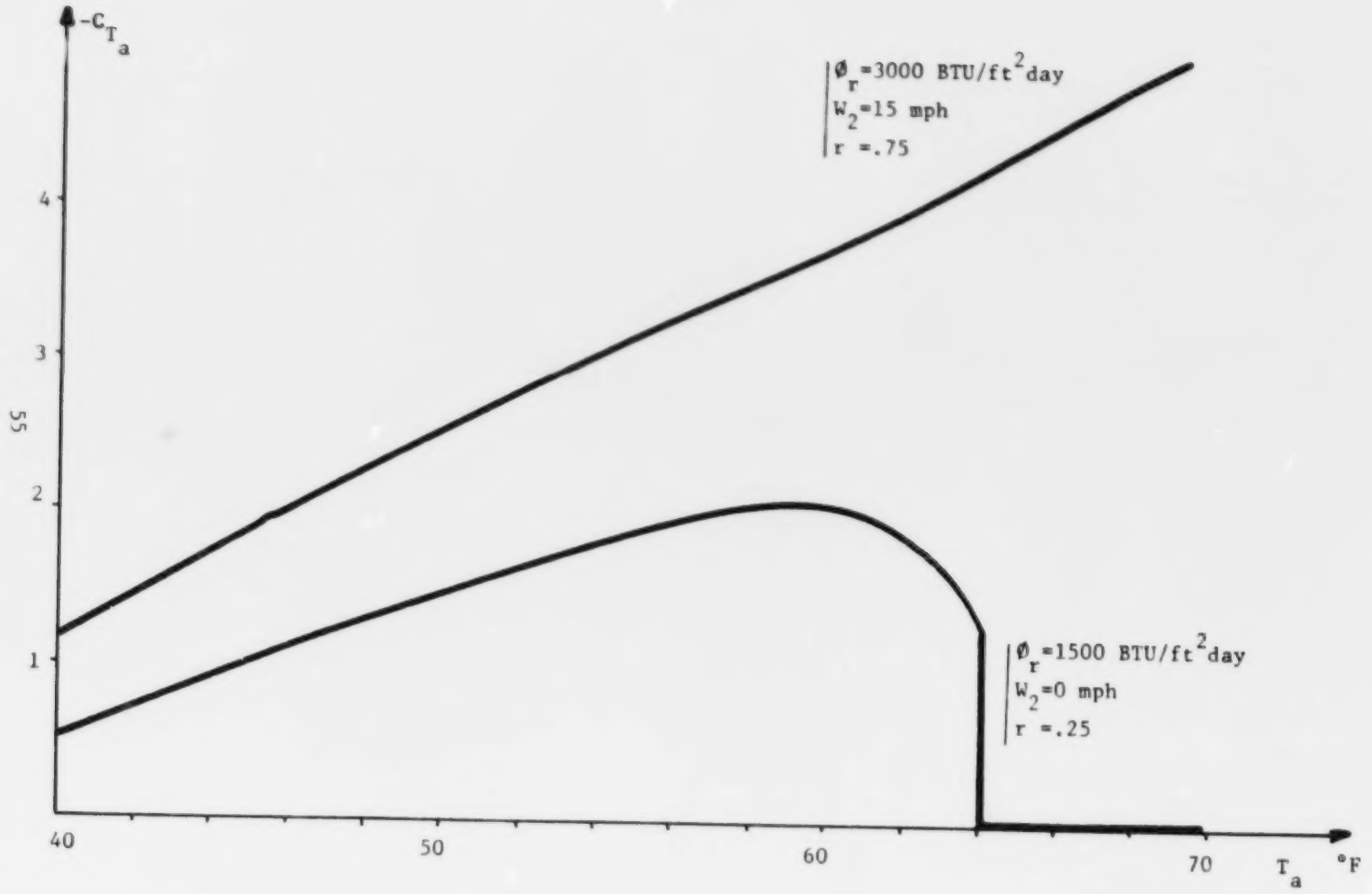

Figure 3-7. Approximate range of variation of the corrolation coefficient for ambiant temperature.

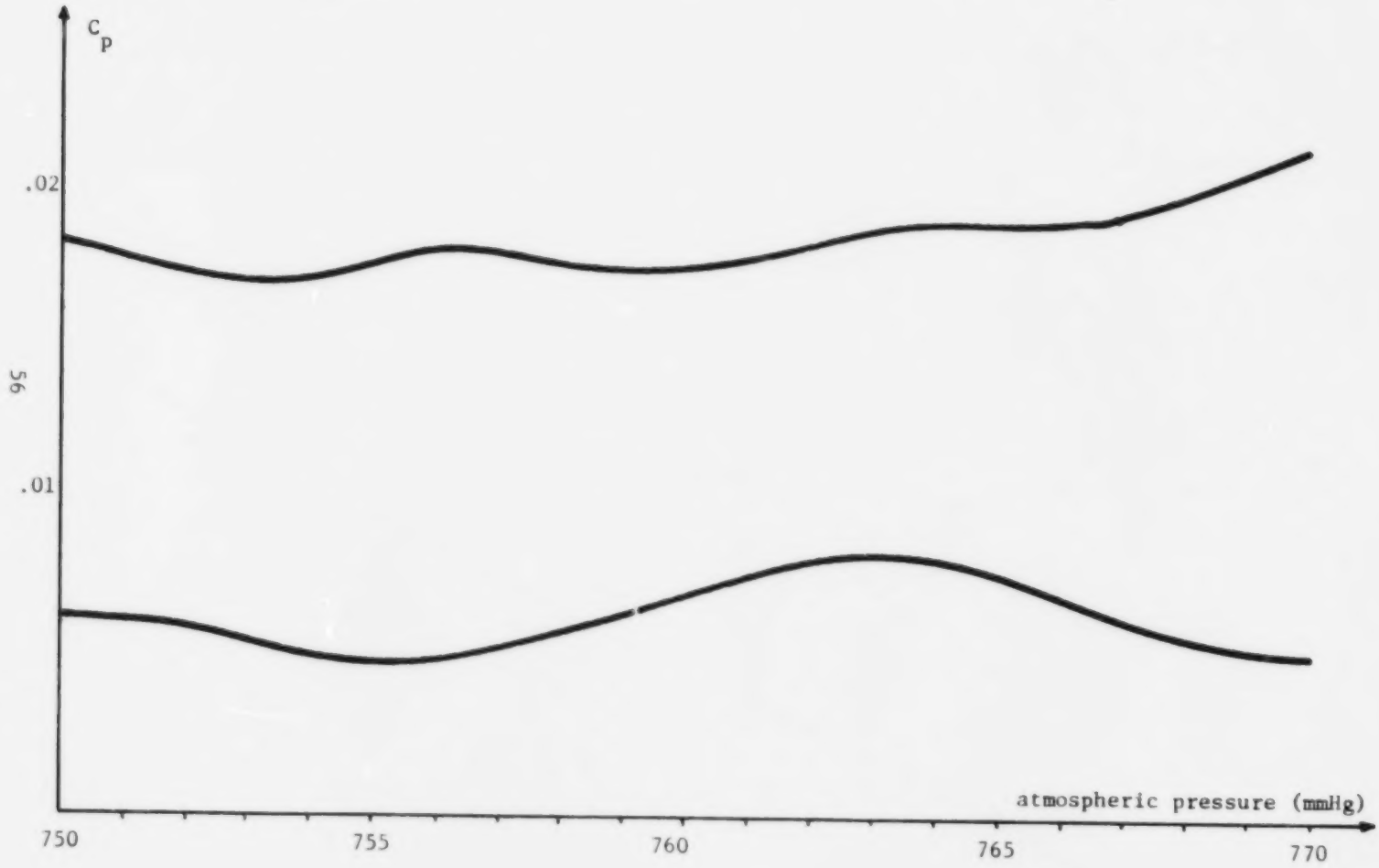

Figure 3-8. Approximate range of variation of the corrolation coefficient for atmospheric pressure.

IV. UNSTEADY MODEL

For highly variable flow conditions, such as in estuaries and reservoirs, the hypotheses made for the steady temperature model described in Chapter 3 are too far from reality to be considered. Taking average flow conditions would damp out the time variation of the local temperature and there is even no certainty that the results obtained would be the average values of the temperature. Moreover, the time variation of the temperature is an important factor since its amplitude can be large and, when an average value would be sustainable for aquatic life, it is possible that the peaks could exceed the lethal limit. The additional stress placed on living organisms by repeated temperature variation is another reason for developing an unsteady model.

If the time variations of the flow characteristics are taken into account, it is also necessary to consider the variability of the meteorological conditions. This is one of the major reasons for modifying the model developed by Dailey and Harleman (1972) which does not allow for such variations.

4.1 Description of Dailey and Harleman's Model

This model is divided into two parts: a hydraulic part and a water quality part. The river or estuary network, which can include tributaries and islands, but no internal control structures or dams, is divided into "reaches" which are connected at "node points". Flow junctions and separations must take place at node points, so that the reaches only contain lateral injections of wastes or lateral inflows whose

characteristics are independent of the flow situation in the reach. So, lateral inflows can account for surface runoff or pumped storage devices but not for tributaries since the discharge of the tributary at the junction is influenced by the discharge of the main flow. A typical estuary network schematization is shown on Figure 4-1 taken from Reference 1.

In the hydraulic part, the equations which govern the flow are solved in order to obtain some of the flow characteristics which are required for the water quality part. Those equations are the continuity equation:

$$\frac{\partial A}{\partial t} + \frac{\partial Q}{\partial x} = q_L \qquad (4\text{-}1)$$

where

A = cross section area of the river or estuary (ft^2)

Q = discharge of the river or estuary (cfs)

q_L = lateral inflow per unit length of the channel (cfs/ft)

and the momentum equation:

$$\frac{\partial}{\partial t}(AU) + \frac{\partial}{\partial x}(QU) = -Ag\left(\frac{\partial z}{\partial x} + \frac{U|U|}{C_z^2 R_h} + \frac{d_c}{\rho}\frac{\partial \rho}{\partial x}\right) \qquad (4\text{-}2)$$

where,

U = cross section averaged velocity = Q/A (ft/sec)

g = acceleration of gravity

C_z = Chezy coefficient

R_h = hydraulic radius of the channel

ρ = fluid density

d_c = depth to the centroid of the channel cross-section

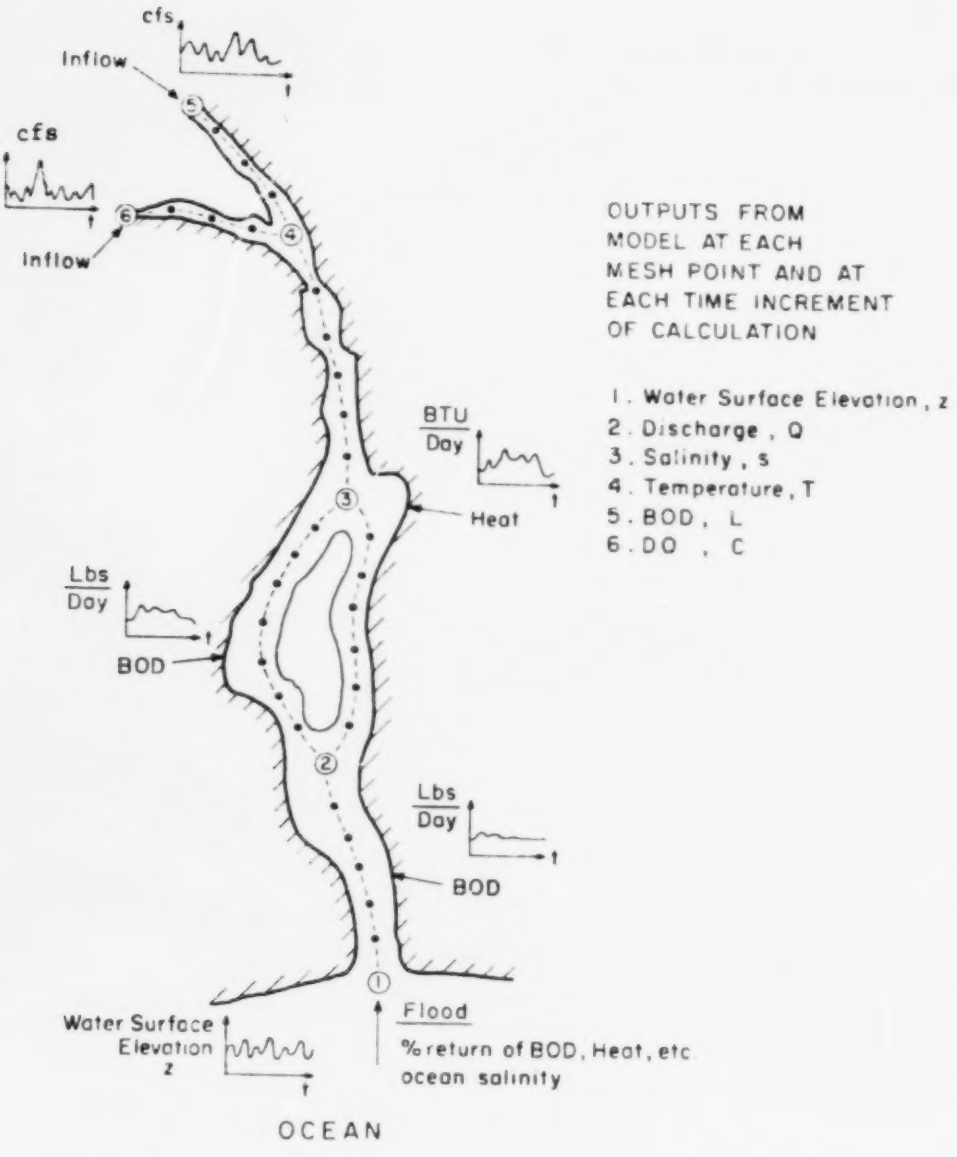

Figure 4.1 Schematic Diagram of a Typical Estuary with Multiple Waste Inputs

The term $- Ag \frac{d_c}{\rho} \frac{\partial \rho}{\partial x}$ accounts for the density variation along the length of the channel. This density variation can be caused by the salinity intrusion but also by a temperature variation. Though, this last effect is not included because of its small magnitude.

This set of partial differential equations can be solved provided one initial condition and two boundary conditions are prescribed. As the model now stands, those initial and boundary conditions can be specified either on the free surface elevation from a fixed horizontal datum or on the discharge. Although other variables could be used such as the average velocity or the cross-sectional area, the elevation and discharge are the more likely to be available from gauge or control structure measurements.

The finite difference scheme used to solve those equations is described in detail in Reference 1 and has not been modified here.

The water quality part solves successively the equation governing the distribution of salinity, temperature, BOD and DO. Our only interest here is in temperature and the corresponding equation in the model is

$$\frac{\partial}{\partial t} (AT) + \frac{\partial}{\partial t} (QT) = \frac{\partial}{\partial x} (AE_L \frac{\partial T}{\partial x}) - K_T A (T - T_E) + S \qquad (4\text{-}3)$$

where S is a source term accounting for waste heat discharges or lateral inflows heat input.

The assumption made of a constant equilibrium temperature T_E both in space and in time allows to write

$$\frac{\partial}{\partial t} (AT_E) + \frac{\partial}{\partial x} (QT_E) = \frac{\partial}{\partial x} (AE_L \frac{\partial T_E}{\partial x}) \qquad (4\text{-}4)$$

since, with $\frac{\partial T_E}{\partial t} = 0$ and $\frac{\partial T_E}{\partial x} = 0$, Equation 4-4 is then equivalent to

$$\frac{\partial}{\partial t} A + \frac{\partial}{\partial x} Q = 0 \qquad (4\text{-}5)$$

which is the continuity Equation (4-1) with $q_L = 0$. This shows that, actually, Dailey and Harleman's model is only valid, for temperature, when $q_L = 0$. In that case, subtracting Equation 4-4 from Equation 4-3 yields

$$\frac{\partial}{\partial t} (A \Delta T_E) + \frac{\partial}{\partial x} (Q \Delta T_E) = \frac{\partial}{\partial x} [AE_L \frac{\partial}{\partial x} (\Delta T_E)] - K_T A \Delta T_E + S \qquad (4\text{-}6)$$

where

$$\Delta T_E = T - T_E$$

In order to later show how the modifications were introduced in the model to account for the variability of the meteorological conditions and for the proportionality of the surface heat flux to the surface area, a summary of the numerical scheme used by Dailey and Harleman to solve Equation 4-6 is now presented. Parts of it are directly taken from the original work (reference 1).

For easier notation let us set $\Delta T_E = c$, and Equation 4-6 becomes

$$\frac{\partial}{\partial t} (Ac) + \frac{\partial}{\partial x} (Qc) - \frac{\partial}{\partial x} (AE_L \frac{\partial c}{\partial x}) + K_T Ac - S = 0 \qquad (4\text{-}7)$$

Each reach is divided into elements which lengths are not necessarily constant and a linear variation of all the terms in Equation 4-7 is assumed over the elements. $(\alpha)_j$ being the value of the variable α at mesh point j, the linear variation is realized by introducing interpolating

functions ϕ_j defined as shown on Figure 4-2, and the linear interpolation for the variable α is realized by the equation

$$\alpha = \sum_{j=1}^{M} \phi_j (\alpha)_j \qquad (4\text{-}8)$$

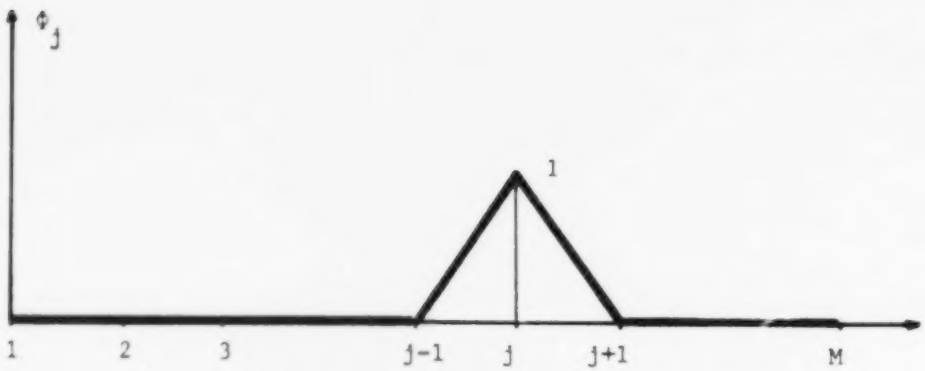

Figure 4-2. Definition of the interpolating function ϕ_j.

Performing this interpolation for all the variables in Equation 4-7 and substituting them in Equation 4-7 yields

$$\frac{\partial}{\partial t}\left[\sum_{j=1}^{M} \phi_j (Ac)_j\right] + \frac{\partial}{\partial x}\left[\sum_{j=1}^{M} \phi_j (Qc)_j\right] - \frac{\partial}{\partial x}\left[\sum_{j=1}^{M} \phi_j \left(AE_L \frac{\partial c}{\partial x}\right)_j\right]$$

$$+ K_T \sum_{j=1}^{M} \phi_j (Ac)_j - \sum_{j=1}^{M} \Phi_j (S)_j = R(x,t) \qquad (4\text{-}9)$$

a residual R(x,t) exists because this piecewise linear approximation does not match exactly the solution.

The method of the weighted residuals is then applied in the form of the Galerkin's method, where the residual is weighted with the

interpolating functions, integrated over the length of the channel and set to zero. This integral can be expressed as a sum of integrals over the elements:

$$\int w_i \, R(x,t) \, dx = \sum_E \int \phi_i \, R(x,t) \, dx = 0 \qquad \text{for } i=1, 2, \ldots, M \quad (4\text{-}10)$$

which now gives M equations with M unknown values of c at each time step. Those equations are

$$\sum_E \int \phi_i \frac{\partial}{\partial t} \left(\sum_{j=1}^{M} \phi_j (Ac)_j \right) dx + \sum_E \int \phi_i \frac{\partial}{\partial x} \left(\sum_{j=1}^{M} \phi_j (Qc)_j \right) dx$$

$$- \sum_E \int \phi_i \frac{\partial}{\partial x} \left(\sum_{j=1}^{M} \phi_j (AE_L \frac{\partial c}{\partial x})_j \right) dx + \sum_E \int \phi_i K_T \sum_{j=1}^{M} \phi_j (Ac)_j \, dx$$

$$- \sum_E \int \phi_i \sum_{j=1}^{M} \phi_j (s)_j \, dx = 0$$

$$i = 1, \ldots, M \qquad (4\text{-}11)$$

A number of approximations are then introduced to transform Equation 4-11 to a more solvable form.

(1) The time derivative of the storage term is approximated as a simple difference:

$$\frac{\partial}{\partial t} (Ac) \approx \sum_{j=1}^{M} \phi_j \frac{\partial}{\partial t} (A_j \bar{c}_j)$$

$$\approx \sum_{j=1}^{M} \phi_j \frac{A_j^{n+1} \bar{c}_j^{n+1} - A_j^n \bar{c}_j^n}{\Delta t} \qquad (4\text{-}12)$$

where

$\bar{c}_j^n$ = discrete value of c at mesh point j at time n

This difference approximates the time derivative best at time

$t + \frac{\Delta t}{2}$ or $(n + \frac{1}{2})\,\Delta t$.

(2) The remaining terms in the equation are approximated also at time $t + \frac{\Delta t}{2}$ by averaging between times t and $t + \Delta t$. For example, the advective term is:

$$\frac{\partial}{\partial x}(Qc) \quad \frac{1}{2}\,\frac{\partial}{\partial x}\left(\sum_{j=1}^{M} \phi_j Q_j^{n+1}\,\bar{c}_j^{n+1} + \sum_{j=1}^{M} \phi_j Q_j^{n}\,\bar{c}_j^{n}\right) \qquad (4\text{-}13)$$

(3) In the dispersion term, the coefficient AE is averaged over each element and c is assumed to vary linearly:

$$AE\,\frac{\partial c}{\partial x} = \frac{1}{2}\left(\overline{AE}^{n+1}\,\frac{\partial}{\partial x}\sum_{j=1}^{M} \phi_j\,\bar{c}_j^{n+1} + \overline{AE}^{n}\,\frac{\partial}{\partial x}\sum_{j=1}^{M} \phi_j\,\bar{c}_j^{n}\right) \qquad (4\text{-}14)$$

where $\overline{AE}$ = average of AE over an element

$$= \frac{1}{2}\left((AE)_j^n + (AE)_{j+1}^n\right) \quad \text{for element } j,\ j+1$$

Assumption (3) is necessary in order to avoid having the dispersive flux integral in Equation (4-11) result in gradients of c rather than value of c themselves at the mesh points. A consequence of this assumption about the dispersive flux is a discontinuity at the mesh points. This discontinuity can be shown by integrating the dispersive flux integral by parts:

$$\int_E \phi_i \frac{\partial}{\partial x}\left(AE \frac{\partial c}{\partial x}\right) dx = \left[\phi_i\, AE \frac{\partial c}{\partial x}\right]_{x_{i-1}}^{x_i} + \left[\phi_i\, AE \frac{\partial c}{\partial x}\right]_{x_i}^{x_{i+1}}$$

$$- \int_E \frac{d\phi_i}{dx}\, AE \frac{\partial c}{\partial x}\, dx \quad i = 1, \ldots, M \tag{4-15}$$

Noting that

$$\phi_i = 0 \text{ at } x = x_{i-1} \tag{4-16a}$$

$$\phi_i = 1 \text{ at } x = x_i \tag{4-16b}$$

$$\phi_i = 0 \text{ at } x = x_{i+1} \tag{4-16c}$$

the terms in brackets are

$$\left.AE \frac{\partial c}{\partial x}\right|_{\substack{x=x_i \\ \text{element } i-1,i}} \qquad - \left.AE \frac{\partial c}{\partial x}\right|_{\substack{x=x_i \\ \text{element } i,\, i+1}} \tag{4-17}$$

= (dispersive flux into element i-1,i)+(dispersive flux into element,i,i+1)

In the physical system this sum is zero; however, it is non-zero in the numerical scheme because of the piecewise linear approximation. Nevertheless, the physics of the system are assumed to prevail, and the sum of the two terms is set to zero, except at the boundaries. There, only one of the terms appears, which corresponds to a natural boundary condition in numerical methods which are based on the calculus of variations.

To simplify the notation, the dispersive fluxes at the boundaries will be written as:

$$-AE \left.\frac{\partial c}{\partial x}\right|_{x=x_1} = \text{dispersive at time } (n+\tfrac{1}{2})\,\Delta t \text{ flux into upstream boundary} \tag{4-18a}$$

$$= \eta_1 \delta_{i1}$$

$$AE \left.\frac{\partial c}{\partial x}\right|_{x=x_M} = \text{dispersive flux at time } (n+\tfrac{1}{2})\Delta t \text{ into downstream boundary} \tag{4-18b}$$

$$= -\eta_M \delta_{iM}$$

where δ_{i1} and δ_{iM} are Kronecker deltas in matrix notation.

Introducing the results of Equations (4-12) through (4-18) into Equations (4-11) yields:

$$\sum_E \int \phi_i \left(\sum_{j=1}^{M} \phi_j A_j^{n+1} c_j^{-n+1}\right) dx + \frac{\Delta t}{2} \sum_E \int \phi_i \left(\sum_{j=1}^{M} \frac{d\phi_j}{dx} Q_j^{n+1} c_j^{-n+1}\right) dx$$

$$+ \frac{\Delta t}{2} \sum_E \overline{AE}_L^{n+1} \int \frac{d\phi_i}{dx} \left(\sum_{j=1}^{M} \frac{d\phi_j}{dx} c_j^{-n+1}\right) dx + \frac{K\Delta t}{2} \sum_E \int \phi_i \left(\sum_{j=1}^{M} \phi_j A_j^{n+1} c_j^{-n+1}\right) dx$$

$$= \sum_E \int \phi_i \left(\sum_{j=1}^{M} \phi_j A_J^n c_j^{-n}\right) dx - \frac{\Delta t}{2} \sum_E \int \phi_i \left(\sum_{j=1}^{M} \frac{d\phi_j}{dx} Q_j^n c_j^{-n}\right) dx$$

$$- \frac{\Delta t}{2} \sum_E \overline{AE}_L^n \int \frac{d\phi_i}{dx} \left(\sum_{j=1}^{M} \frac{d\phi_j}{dx} c_j^{-n}\right) dx - \frac{K\Delta t}{2} \sum_E \int \phi_i \left(\sum_{j=1}^{M} \phi_j A_j^n c_j^{-n}\right) dx$$

$$+ \eta_1 \Delta t\, \delta_{i1} - \eta_M \Delta t\, \delta_{iM} + \Delta t \sum_E \phi_i S^{n+\frac{1}{2}} dx, \quad i = 1, \ldots M \tag{4-19}$$

Appendix A contains a summary of the values of the integrals in Equations (4-19). With these values, Equations (4-19) may be written in matrix notation as:

$$\underline{\underline{A}}\,\underline{c}^{n+1} = \underline{\underline{D}}\,\underline{c}^{n} + \underline{e} \qquad (4\text{-}20)$$

The coefficient matrices $\underline{\underline{A}}$ and $\underline{\underline{D}}$ are defined in such a way as to emphasize their tri-diagonal nature. To save notation and execution time in the computer, the individual matrix elements are evaluated in terms of certain factors which can be calculated once and used repetitively thereafter.

$$\underline{\underline{A}} = \begin{bmatrix} a^1 & c^1 & & & & \\ b^2 & a^2 & c^2 & & & \\ & \ddots & \ddots & \ddots & & \\ & & & b^{M-1} & a^{M-1} & c^{M-1} \\ & & & & b^{M} & a^{M} \end{bmatrix}$$

where

$$a^1 = 2f_2\,\Lambda_{1,2}\,A_1^{n+1} - f_4^{1,n+1} + f_1^{1,n+1}$$

$$a^i = 2f_2(\Lambda_{i-1,i} + \Lambda_{i,i+1})A_i^{n+1} + f_1^{i-1,n+1} + f_1^{i,n+1}, \quad 2 \le i \le M-1$$

$$a^M = 2f_2\,\Lambda_{M-1,M}\,A_M^{n+1} + f_4^{M,n+1} + f_1^{M-1,n+1}$$

$$c^i = f_2\,\Lambda_{i,i+1}\,A_{i+1}^{n+1} + f_4^{i+1,n+1} - f_1^{i,n+1}, \quad 1 \le i \le M-1$$

$$b^i = f_2\,\Lambda_{i-1,i}\,A_{i-1}^{n+1} - f_4^{i-1,n+1} - f_1^{i-1,n+1}, \quad 2 \le i \le M$$

and

$$f_1^{i,n+1} = \frac{A_i^{n+1} E_i^{n+1} + A_{i+1}^{n+1} E_{i+1}^{n+1}}{\Delta_{i,i+1}} \frac{\Delta t}{4}$$

$$f_2 = \frac{1}{6}\left(1 + \frac{K\Delta t}{2}\right)$$

$$f_3 = \frac{1}{6}\left(1 - \frac{K\Delta t}{2}\right)$$

$$f_4^{i,n+1} = \frac{Q_i^{n+1} \Delta T}{4}$$

$$\underline{D} = \begin{bmatrix} d_a^1 & d_c^1 & & & & \\ d_b^2 & d_a^2 & d_c^2 & & & \\ & \ddots & \ddots & \ddots & & \\ & & & d_b^{M-1} & d_a^{M-1} & d_c^{M-1} \\ & & & & d_b^M & d_a^M \end{bmatrix}$$

where

$$d_a^1 = 2f_3 \Delta_{1,2} A_1^n + f_4^{1,n} - f_1^{1,n}$$

$$d_a^i = 2f_3 (\Delta_{i-1,\,i} + \Delta_{i,\,i+1}) A_i^n - f_1^{i-1,n} - f_1^{i,n}, \quad 2 \le i \le M-1$$

$$d_a^M = 2f_3 \Delta_{M-1,M} A_M^n - f_4^{M,n} - f_1^{M-1,n}$$

$$d_c^i = f_3 \Delta_{i,i+1} A_{i+1}^n - f_4^{i+1,n} + f_1^{i,n}, \quad 1 \le i \le M-1$$

$$d_b^i = f_3 \Delta_{i-1,i} A_{i-1}^n + f_4^{i-1,n} + f_1^{i-1,n}, \quad 2 \leq i \leq M$$

The vectors $\underline{\bar{c}}$ and $\underline{e}$ are defined as:

$$\underline{\bar{c}}^n = \begin{bmatrix} \bar{c}_1 \\ \bar{c}_2 \\ \\ \bar{c}_{M-1} \\ \bar{c}_M \end{bmatrix} \qquad \underline{e} = \begin{bmatrix} \eta_1 \Delta t + (\text{source terms})_1 \\ (\text{source term})_2 \\ \\ (\text{source terms})_{M-1} \\ -\eta_M \Delta T + (\text{source terms})_M \end{bmatrix}$$

Initial and Boundary Conditions

The set of M linear equations represented by Equation 4-20 is solved at each time step to give the temperature profile ($\underline{\bar{c}}^{n+1}$) given the one Δt before ($\underline{\bar{c}}^n$). It is then necessary, in order to start the computation to specify the initial temperature profile ($\underline{\bar{c}}^1$).

Though, Equation 4-20 contains M+2 unknowns: the values of c at each of the M meshpoints and the two extreme dispersive fluxes, $\eta_1 \Delta t$ and $\eta_2 \Delta t$; and 2 of them are to be specified as boundary conditions, at all times, to allow the resolution of the system. The easiest choice would seem to be the 2 dispersive fluxes, but their determination requires the knowledge of the extreme temperature gradients, which are, in the general case, more difficult to obtain than the temperatures themselves. So the program is set to handle both types of boundary conditions.

4.2 Modification of Dailey and Harleman's Model

The exact equation for one-dimensional, unsteady heat transfer

is Equation 2-1 and assuming the product ρc to be constant over the range of temperatures considered yields

$$\frac{\partial}{\partial t}(AT) + \frac{\partial}{\partial x}(QT) = \frac{\partial}{\partial x}\left(AE_L \frac{\partial T}{\partial x}\right) + \frac{b\phi_n}{\rho c} + \frac{WHD + THD}{\rho c} \qquad (4\text{-}21)$$

and it is easy to check that $\frac{WHD + THD}{\rho c}$ is equal to the source term S used in Equation 4-3.

If we consider the meteorological conditions as variable with time, Equation 4-4 is no longer valid and the linearization of the surface heat flux does not bring any simplification since ΔT_E cannot be isolated. Moreover, if the model is to be run for long periods of time during which the water temperature varies greatly, the dependence of the water temperature on K has to be taken into account. So, it was chosen here to directly determine the net surface heat flux ϕ_n through Equation 2-24 at each meshpoint and time step.

Equation 4-21 is similar to the one solved in Dailey and Harleman's model (Equation 4-7) from which it differs only by the flux term. It was not thought necessary to write a new program.

In order to keep as much as possible the structure of the original program, the decay term was simply eliminated by setting the decay coefficient to zero in the data set; and the new value of the surface heat flux was introduced as a supplementary term.

Keeping consistent with the original numerical scheme, a piecewise linear interpolation of b and ϕ_n is performed between the mesh points.

$$\frac{b\phi_n}{\rho c} = \frac{1}{\rho c} \sum_{j=1}^{M} \Phi_j (b\phi_n)_j$$

and Equation 4-11 becomes

$$\sum_E \int \phi_i \frac{\partial}{\partial t} \left(\sum_{j=1}^{M} \phi_j (Ac)_j \right) dx + \sum_E \int \phi_i \frac{\partial}{\partial x} \left(\sum_{j=1}^{M} \phi_j (Qc)_j \right) dx$$

$$- \sum_E \int \phi_i \frac{\partial}{\partial x} \left(\sum_{j=1}^{M} \phi_j (AE_L \frac{\partial c}{\partial x})_j \right) dx - \frac{1}{\rho c} \sum_E \int \phi_i \sum_{j=1}^{M} \phi_j (b\emptyset_n)_j \, dx$$

$$- \sum_E \int \phi_i \sum_{j=1}^{M} \phi_j (S)_j \, dx = 0 \qquad i = 1, \ldots, M \qquad (4\text{-}22)$$

where c now stands for T.

According to hypothesis (2) previously stated, the new term should be approximated at time $t + \frac{\Delta t}{2}$. It should be noted that there is no rational for taking $t + \frac{\Delta t}{2}$ rather than any other value in the segment $[t , t+\Delta t]$ except simplicity, but this approximation was conserved here because an iteration would require a complete change of the structure of the program.

This approximation is

$$\sum_E \int \phi_i \sum_{j=1}^{M} [\phi_j (b\emptyset_n)_j] \, dx \simeq \frac{1}{2} \sum_E \int \phi_i \sum_{j=1}^{M} [\phi_j (b\emptyset_n)_j^n] \, dx$$

$$+ \frac{1}{2} \sum_E \int \phi_i \sum_{j=1}^{M} [\phi_j (b\emptyset_n)_j^{n+1}] \, dx \qquad (4\text{-}23)$$

Though $\emptyset_n$ is unknown at time $(n+1)\,\Delta t$ since it depends on the water temperature at that time which is what is being calculated, and the functional relationship between $\emptyset_n$ and the temperature is too complicated to allow an implicit resolution. So, the temperature is taken at time $n\,\Delta t$ only, which gives

$$(\phi_n)_j^{n+1/2} = \frac{1}{2}\left[\phi_n(MC_j^n,\ T_j^n) + \phi_n(MC_j^{n+1},\ T_j^n)\right] \qquad (4\text{-}24)$$

which is furthermore approximated to

$$(\phi_n)_j^{n+1/2} = \phi_n\left(\frac{MC_j^n + MC_j^{n+1}}{2},\ T_j^n\right) \qquad (4\text{-}25)$$

so that Equation 4-23 can be approximated by

$$\sum_E \int \psi_i \sum_{j=1}^{M} \left[\psi_j (b\phi_n)_j\right] dx = \sum_E \int \psi_i \sum_{j=1}^{M} \psi_j \left[\frac{b_j^n + b_j^{n+1}}{2}\ \phi_n\left(\frac{MC_j^n + MC_j^{n+1}}{2},\ T_j^n\right)\right] dx \qquad (4\text{-}26)$$

and the new form of Equation 4-19 is

$$\sum_E \int \psi_i \left(\sum_{j=1}^{M} \psi_j\ A_j^{n+1}\ \bar{c}_j^{n+1}\right) dx + \frac{\Delta t}{2} \sum_E \int \psi_i \left(\sum_{j=1}^{M} \frac{d\psi_j}{dx}\ Q_j^{n+1}\ \bar{c}_j^{n+1}\right) dx$$

$$+ \frac{\Delta t}{2} \sum_E \overline{AE}_L^{n+1} \int \frac{d\psi_i}{dx} \left(\sum_{j=1}^{M} \frac{d\psi_j}{dx}\ \bar{c}_j^{n+1}\right) dx = \sum_E \int \psi_i \left(\sum_{j=1}^{M} \psi_j A_j^n\ \bar{c}_j^n\right) dx$$

$$- \frac{\Delta t}{2} \sum_E \int \psi_i \left(\sum_{j=1}^{M} \frac{d\psi_j}{dx}\ Q_j^n\ \bar{c}_j^n\right) dx - \frac{\Delta t}{2} \sum_E \overline{AE}_L^n \int \frac{d\psi_i}{dx} \left(\sum_{j=1}^{M} \frac{d\psi_j}{dx}\ \bar{c}_j^n\right) dx$$

$$+ \frac{\Delta t}{\theta} \sum_E \int \psi_i \sum_{j=1}^{M} \psi_j \left[\frac{b_j^n + b_j^{n+1}}{2}\ \phi_n\left(\frac{MC_j^n + MC_j^{n+1}}{2},\ \bar{c}_j^n\right)\right] dx$$

$$+ \alpha_1 \Delta t\ \delta_{i1} - \alpha_M \Delta t\ \delta_{iM} + \Delta t \sum_E \int \psi_i\ S^{n+1/2}\ dx \qquad i = 1, \ldots, M \qquad (4\text{-}27)$$

which can be written in matrix notation

$$\underline{\underline{A}}\ \underline{\bar{c}}^{n+1} = \underline{\underline{D}}\ \underline{\bar{c}}^n + \underline{e} + \underline{f}^{n+1/2} \qquad (4\text{-}28)$$

where $\underline{\underline{A}}$, $\underline{\underline{c}}^{n+1}$, $\underline{\underline{D}}$, $\underline{\underline{c}}^{n}$ and $\underline{e}$ are the same as in Equation 4-20, with K = 0, and $\underline{f}^{n+1/2}$ accounts for the new shape of the surface heat flux term. Taking the correct values for the integrals, as given in Appendix A, the elements of the new matrix $\underline{f}$ are

$$f_1^{n+1/2} = \left[\frac{\Delta_{1,2}}{3} (\phi_n b)_1^{n+1/2} + \frac{\Delta_{1,2}}{6} (\phi_n b)_2^{n+1/2} \right] \frac{\Delta t}{\rho c}$$

$$f_1^{n+1/2} = \left[\frac{\Delta_{i-1,i}}{6} (\phi_n b)_{i-1}^{n+1/2} + \frac{(\Delta_{i-1,i} + \Delta_{i,i+1})}{3} (\phi_n b)_i^{n+1/2} \right.$$

$$\left. + \frac{\Delta_{i,i+1}}{6} (\phi_n b)_{i+1}^{n+1/2} \right] \frac{\Delta t}{\rho c}$$

$$f_M^{n+1/2} = \left[\frac{\Delta_{M-1,M}}{6} (\phi_n b)_{M-1}^{n+1/2} + \frac{\Delta_{M-1,M}}{3} (\phi_n b)_M^{n+1/2} \right] \frac{\Delta t}{\rho c} \qquad (4\text{-}29)$$

The initial and boundary condition requirements are the same as in the original version of the model.

4.3 Test Run

In order to test the modification introduced, a run was made for a steady situation with the same conditions as in the sample run of the steady model described in Chapter 3. The flow characteristics needed for the steady model were the discharge (taken as 1000 cfs) and the width (taken as 1000 ft). For the unsteady model, since the hydraulics are computed through the continuity and momentum equations, more geometrical data is required. The depth was chosen as 5 ft. which gives a cross-section averaged velocity of 0.2 ft/sec. The required Manning's coefficient was chosen as 0.02 and the slope was computed through the Manning's

equation to be $0.854\ 10^{-6}$ to ensure a constant depth with distance.

The meteorological conditions are the same as for the sample run of the steady model, namely

$$T_a = 60°F$$

$$r = .75$$

$$\phi_r = 2500\ BTU/ft^2\ day$$

$$p = 760\ mm\ Hg$$

and the corresponding equilibrium temperature is 52.8°F. The dispersive coefficient is internally computed through the Taylor equation

$$E_L = 77\ n\ U\ R_h^{5/6} \qquad (4-30)$$

where n is the Manning's coefficient.

The upstream boundary condition was specified on the temperature itself (61.4°F) and the downstream boundary was specified on the dispersive flux which is imposed to be zero. This implies a zero slope of the temperature profile at the downstream boundary which is not totally exact since the temperature decay continues to infinity, but this condition allows a better verification than imposing the temperature at the downstream end from the results of the steady model. The length of the portion under study was chosen to be long enough to allow an almost zero slope of the temperature profile, and thus approximate better the downstream boundary condition.

The initial condition was chosen as 58°F all over the 50,000 ft. of the river portion under study.

This run describes the evolution of the temperature profile

in a river initially at uniform temperature (58°F) larger than the equilibrium (52.8°F) in which, from time t = 0 onwards, the upstream incoming water is at 61.4°F. The temperature profiles after 1, 2 and 3 days given by the unsteady model are plotted on Figure 4-3 which shows the simultaneous progression of the hot water front and the general temperature decay.

The mean velocity being 0.2 ft/sec., at time 265200 s (3 days), the hot water front traveled approximately 53,040 ft. and a steady state should be reached. This is verified as the temperature profile after 3 days matches almost perfectly the one given by the steady model.

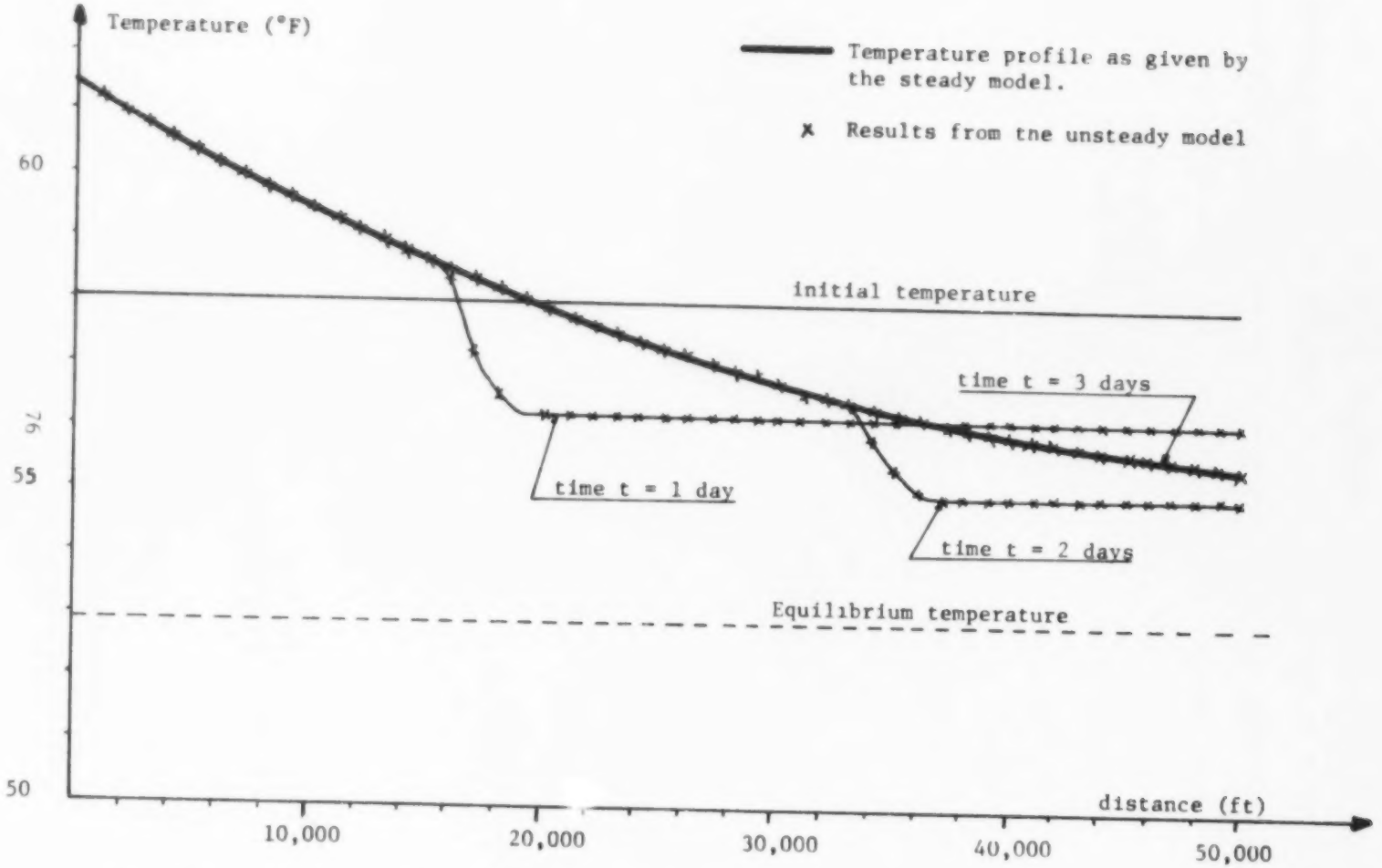

Figure 4-3. Test run with steady river parameters and meteorological conditions.

V. CASE STUDY: CONOWINGO RESERVOIR

5.1 Natural Temperature Distributions

The ability of the modified version of Dailey and Harleman's model to predict temperatures as a function of distance and time under varying meteorological conditions was tested on the Conowingo Reservoir, located on the Susquehanna River at the border between Pennsylvania and Maryland. This reservoir, a map of which is shown in Figure 5-1, is situated between Holtwood Dam at the upstream end and Conowingo Dam at the downstream end. The reservoir is also the site of the Peach Bottom Atomic Power Station and of the Muddy Run Pumped Storage Generating Plant. The flow in the reservoir is governed by the operation of the hydroelectric dams and pumped storage plant, so that it is highly unsteady and reversals of the flow direction occur at frequent intervals.

The modified mathematical model was applied to determine the natural temperature distribution in the reservoir as a function of time. Natural temperature refers to the temperature in the absence of heat addition by condenser water discharge from the Peach Bottom Atomic Power Station.

Because of the one-dimensional nature of the mathematical model in which $T = f(x,t)$, the calculated temperature at any given time and distance corresponds to the temperature averaged over the cross-section of the reservoir. Observations of natural temperatures in Conowingo Reservoir show that, except for a short period in late summer, there is relatively little temperature stratification. This is especially true in the upper portion of the reservoir where the average depth is less than 20 feet. Thus the utilization of the transient, longitudinal temperature distribution model seems to be justified.

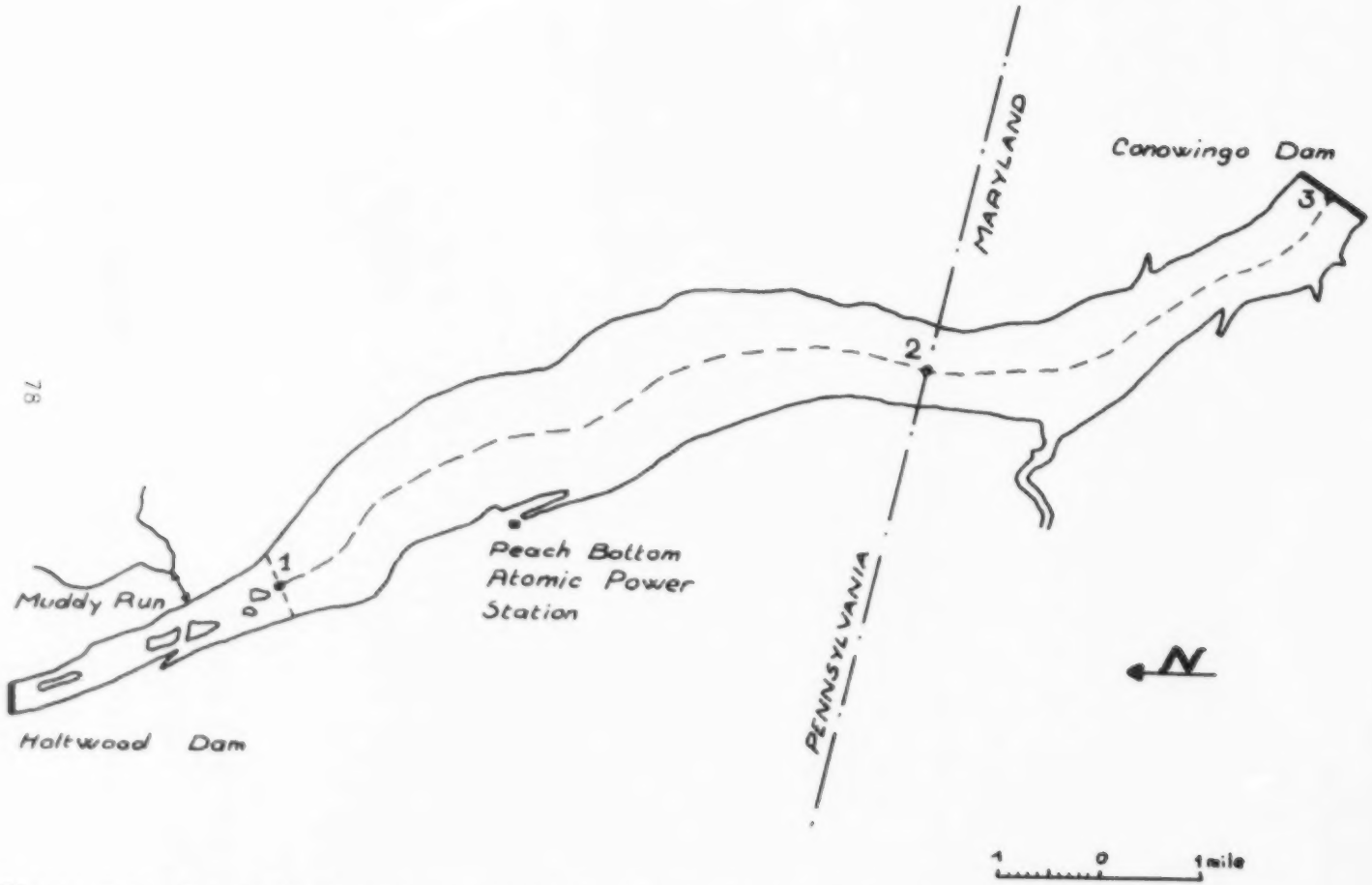

Figure 5-1. Map of the Conowingo reservoir showing the schematization used for the model.

The predictive qualities of the model are required by the ultimate aim of the study which is to determine the temperature excess over the natural due to the operation of the atomic power plant. For that purpose the model will compute the natural temperature, given the meteorological conditions and boundary conditions independent of the heated water discharge. The temperature excess will be determined by subtracting the calculated natural temperatures from the measured temperatures in the reservoir during operation of the power plant.

The portion of the reservoir in which the temperature distribution is of primary interest is between the upstream end and the state line. Therefore, the reservoir was divided into two reaches with a junction node on the state line, as shown on Figure 5-1. It was necessary to extend the model to Conowingo Dam in order to have adequate downstream boundary conditions. The upstream boundary (node 1) was shifted south from Holtwood Dam, to the point where the lake proper begins, to avoid a section of very shallow water which contains cascades and supercritical flows and for which the hydraulic part of the model cannot be applied because of limited topographical information.

For the hydraulic part, the mesh spacing was chosen as 1500 ft. and the time step as 720 sec. The discharge versus time was specified as the upstream boundary condition (node 1) equal to the sum of the discharges from Holtwood Dam and Muddy Run Pumped Storage Plant. In this sum the discharge from Muddy Run was taken as positive or negative according to whether the water is flowing into or pumped from the reservoir. The downstream boundary (node 3) was specified on the elevation as a function of time at Conowingo Dam. All the data for the hydraulic part was taken from the operating schedules of the dams and pumped storage plant.

For the temperature computations the mesh spacing was chosen as 500 ft. and the time step as 720 sec. The upstream boundary condition was specified as the temperature versus time, when the direction of the flow was downstream at node 1 and as the dispersive heat flux, $AE_L \frac{\partial T}{\partial x}$, when the flow direction was reversed. In the latter case the dispersive flux is computed at each time step as well as an esimtate of its variation rate, thus allowing an approximation of its value at the next time step which is used as boundary condition. This type of boundary condition, which is similar to the one used at the ocean entrance in the case of an estuary, was taken to ensure future independence of the boundary condition from the heated water discharge of the power plant. Otherwise, when the flow reverses, the influence of the heat source due to the power plant may reach the upstream boundary and the subsequently computed temperature distribution would not be the natural one. The original model provides for such a boundary condition, but the incoming temperature is specified as constant with time and a change had to be made to allow for the temporal variation. The downstream boundary condition was specified on the dispersive flux of heat which is imposed as zero because of the presence of the dam which breaks continuity and only allows advection. The longitudinal dispersion coefficient E_L was chosen as 100 times the Taylor value as given by Equation 4-30, to obtain the best compromise between exactitude of the results and stability of the numerical scheme for the longitudinal temperature profiles. Such a ratio is well in accordance with measurements made on the Mississippi River and reported by Yotsukura (1967) which show that for high values of the width to depth ratio (about 300 in our case) the longitudinal dispersion coefficient can be as high as 200 times the Taylor value. Large values of the longitudinal dispersion coefficient

also tend to smooth the numerical instabilities in the temperature profiles as can be seen by comparing Figures 5-7 and 5-8 which show the computed profiles on September 2, 1972 at 24 hours with dispersion coefficients equal to 100 and 10 times the Taylor value.

Two runs of the model were made; one for a period of 3 days starting August 31, 1972 at 24 hours (Julian day 235) and ending September 3, 1972 at 24 hours (Julian day 238); and the other one for a period of 18 days starting April 7, 1972 at 24 hours (Julian day 93) and ending April 25 at 24 hours (Julian day 116). These periods were chosen due to the availability of measurements to provide boundary conditions and to check the results of both the hydraulic and temperature predictions of the model.

Plots of the outputs of the model for reach 1 are given on Figures 5-2 to 5-8 for the September run and 5-9 to 5-13 for the April run. The results for reach 2 are generally not given as insufficient measurements were available to allow a verification. For both runs, extremely good correlation is obtained for the hydraulic part as can be seen from Figures 5-2, 5-9 and 5-10. Unfortunately, the only measurements available were that of the centerline surface velocity which is not strictly equal to the cross-section averaged value computed by the one-dimensional model.

The results of the thermal part of the model are also in good agreement with the measurements. Though, for the September run the computed values become lower than the measured ones as time increases. This can be explained by the fact that the measurements were made very near the surface whereas the model determines cross-section averaged temperatures. More thorough measurements made during that same period of time show that, in effect, the temperature decreases with depth. In reach 1, where the depth varies between 12 and 19 feet, the temperature difference between the surface and the bottom

can be as high as 2°F. Unfortunately the time of the measurements at varying depths was not recorded with sufficient precision to allow a verification of the average temperatures; but the computed values are well within the probable range, since the difference between the computed cross-section averaged temperature and the measured surface temperature rarely exceeds 1°F. The fact that this difference increases with time at the beginning of the run is due to the specification of the initial condition which was made on the surface temperature. For the April run, where the correlation is better, measurements at various depths show that the vertical temperature gradients are much lower.

Another cause for differences between observed and calculated temperatures is the fact that temperature measurements at the upstream boundary were not available and, when this boundary condition is specified on temperature (flow in the downstream direction), the data from the nearest monitoring station, situated some 8000 ft. downstream, was used.

Figure 5-3, which shows the variation with time of the temperature at the upstream boundary for the September run, proves the validity of the boundary condition used when the direction of flow reverses. Except during the first flow reversal, which is also the beginning of the run, the computed temperature matches the measured one very well. The discrepancy during the first reversal comes from the fact that the dispersive flux, which is used as a boundary condition, is computed from the initial condition which is somewhat imprecise because of the limited number of monitoring stations.

As in many mathematical model verifications, the available data, although very extensive, proved to be partially inadequate in providing all

the information required to run the model and to precisely check its results. This is due to the fact that the characteristics which can be determined with simplicity by measurement and by mathematical models are rarely the same and judgement has to be used in their interpretation. In this case study of the Conowingo Reservoir, distortions are introduced in the results because of the lack of temperature measurements at the location which was dictated as the upstream boundary by modeling considerations, and verification is influenced by the fact that only surface temperature measurements were generally available.

Despite these limitations, it is felt that good agreement exists between the results of the model and the image of the physical reality which can be derived from the available measurements.

5.2 Effect of Waste Heat Input

The condenser water discharge structure for Unit No. 2 of the Peach Bottom Atomic Power Station is a surface channel entering the reservoir almost parallel to the shoreline. It is expected that the heated water plume will remain attached to the side thus creating significant transverse temperature gradients. Although the mathematical model described herein can include artificial heat injections, the one-dimensional nature of the model, which assumes complete mixing of the heated effluent across the section of the reservoir adjacent to the outfall, is not realistic in this situation. Because of the interest in the near field excess temperature distribution, the procedure outlined in section 5-1 was chosen. Since the lateral gradients of the natural temperature are generally very small, the excess temperature can be computed by subtraction of the computed natural temperature from the measured temperature once the power

plant is operating. This procedure should be fairly accurate even in the near field region of the outfall structure.

The complete mixing hypothesis inherent in the one-dimensional model theoretically gives the least local temperature increases and as such is an interesting limiting case. Additional runs of the model were carried out taking into account the waste heat input from Unit 2 of the Peach Bottom Atomic Power Station (discharge 1650 cfs, excess temperature 20.8°F). Figures 5-14 and 5-15 show the resulting excess temperature profiles at different times of the day in April and September. The mean daily flow through the reservoir during April is about five times larger than in September. This explains the fact that peak excess temperaturesat the power plant output location are higher in September than in April. The larger excess temperatures in the reservoir upstream of the plant in September are explained by the fact that flow reversals are common during this period, whereas, during April the flow is essentially unidirectional. The differences in the profiles at different times of the day, especially in April, show the importance of a transient model where both flow characteristics and meteorological conditions vary with time.

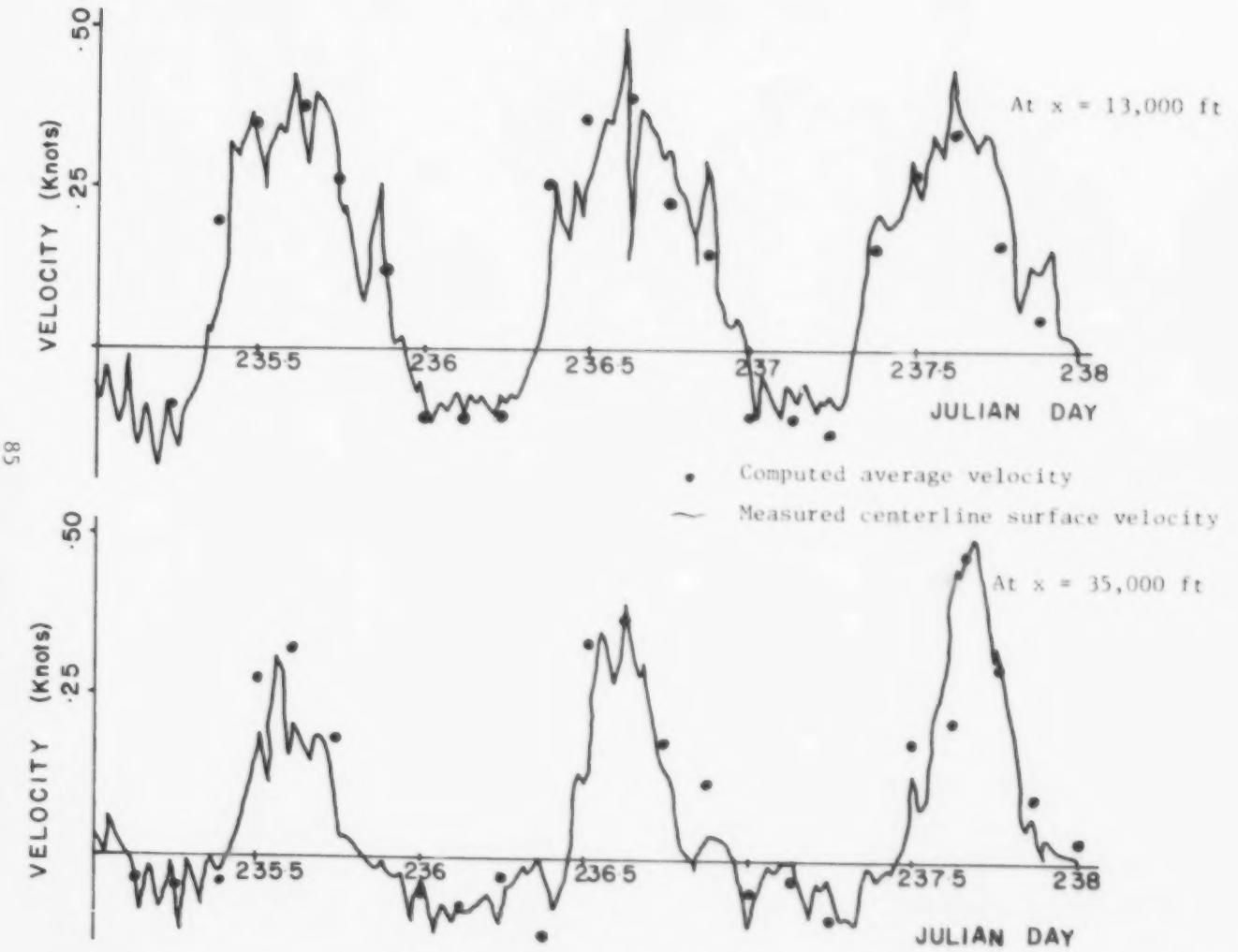

Figure 5-2: Time variations of the velocity from September 1st to 3rd, 1972 at two locations in Conowingo Reservoir.

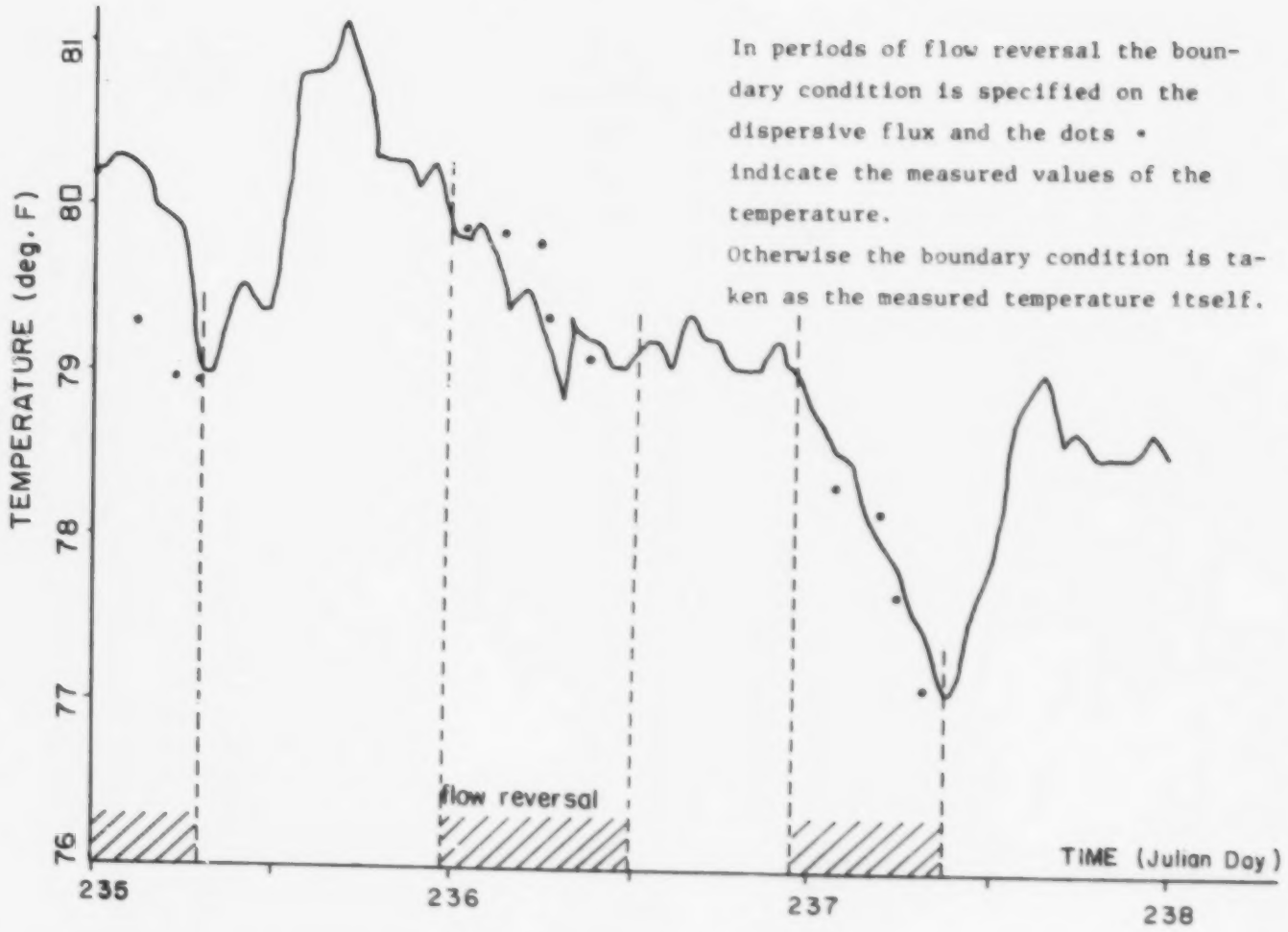

Figure 5-3: Time variations of the temperature from September 1st to 3rd, 1972 at the upstream end of Conowingo Reservoir.

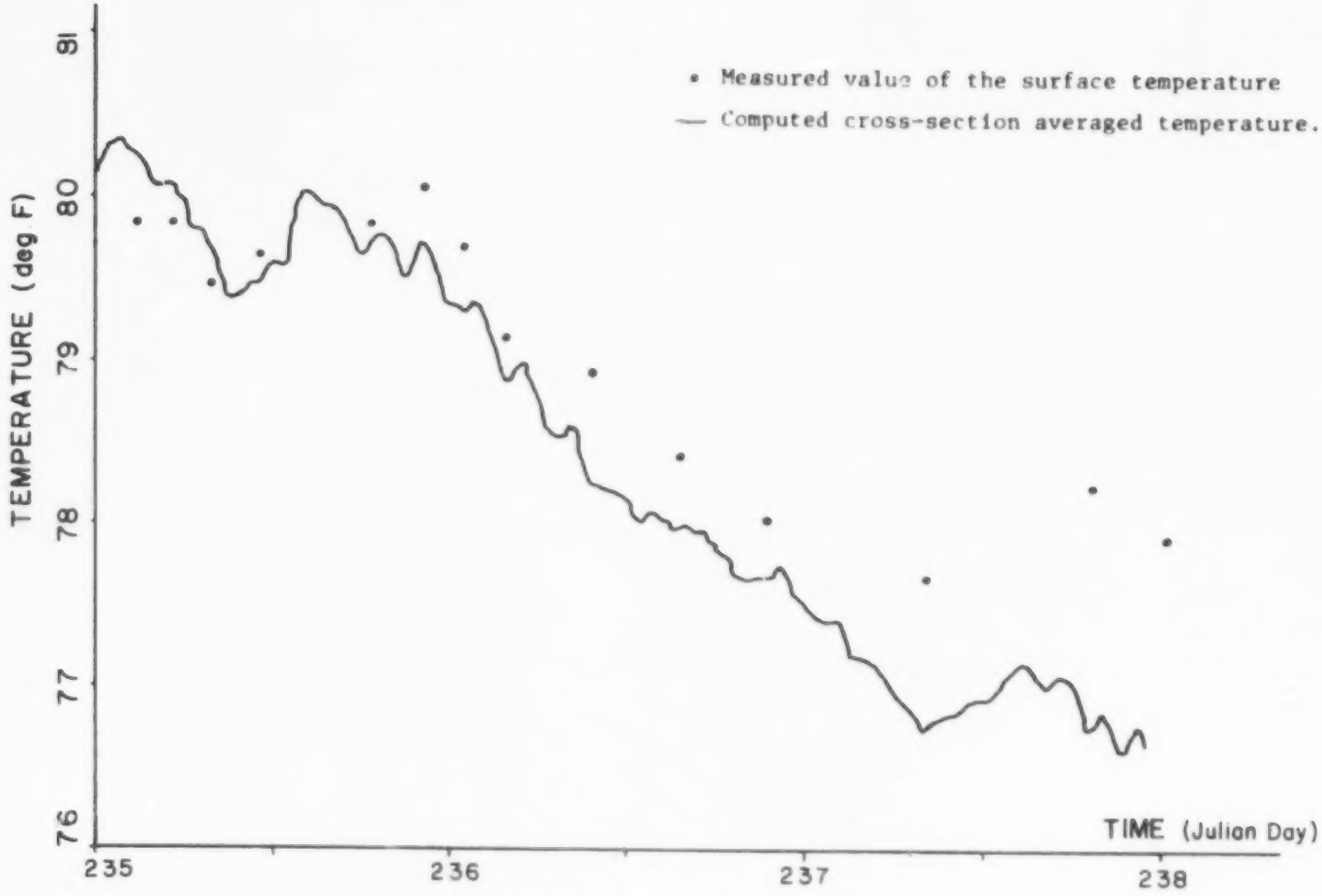

Figure 5-4: Time variations of the temperature from September 1st to 3rd, 1972 at x = 19,000 ft. in Conowingo Reservoir.

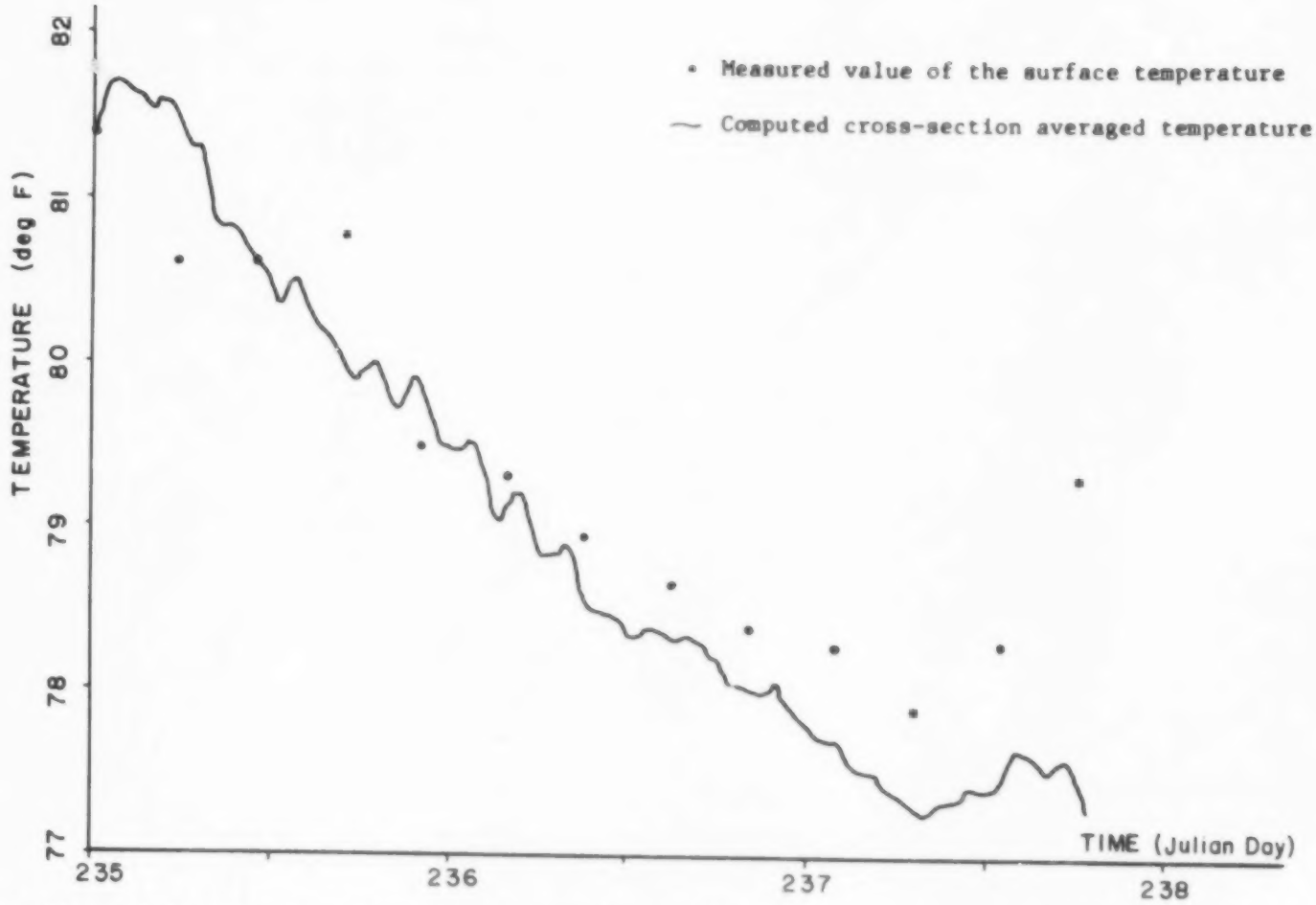

Figure 5-5: Time Variations of the temperature from September 1st to 3rd, 1972 at x = 27,500 ft. in Conowingo Reservoir.

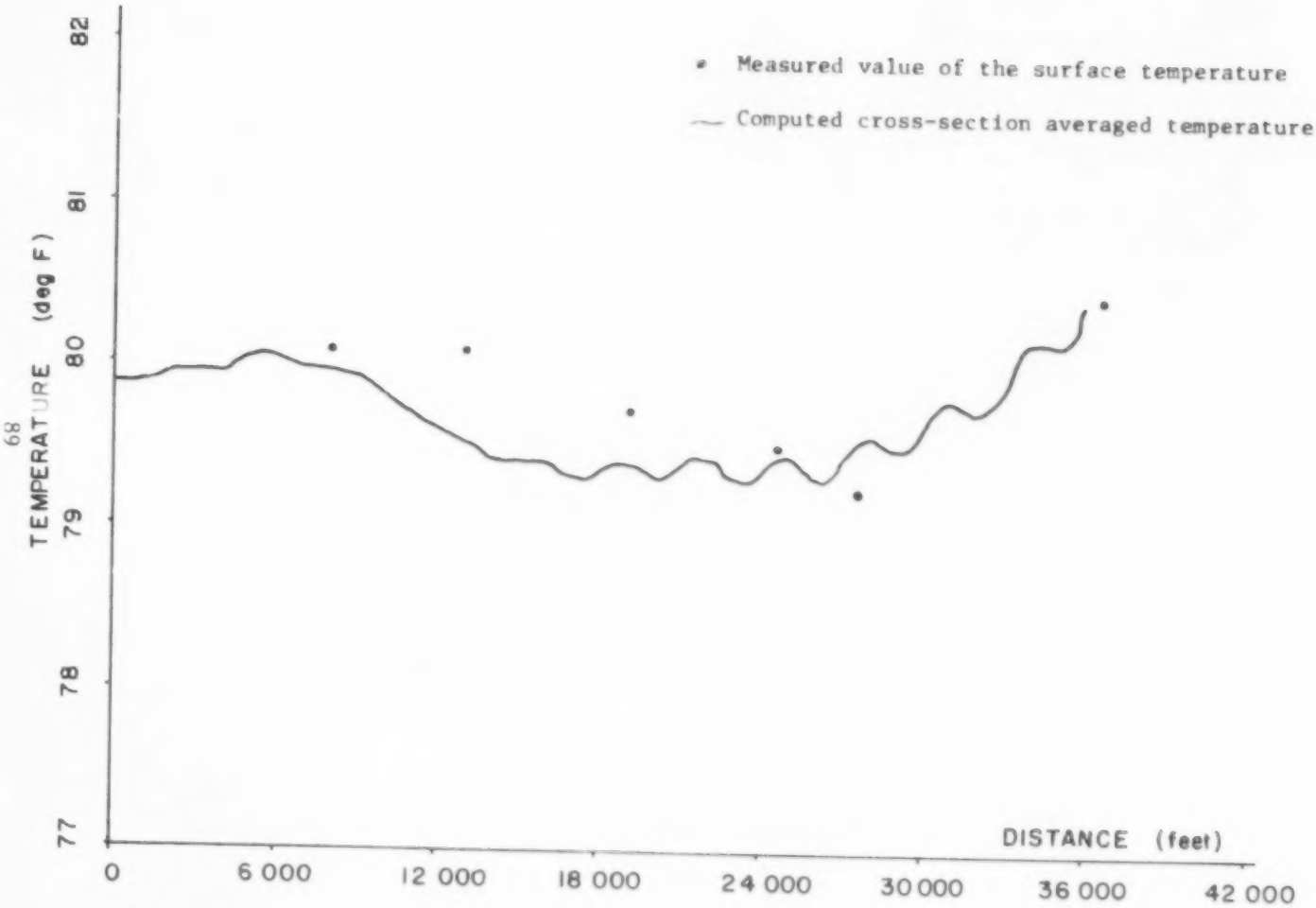

Figure 5-6: Temperature profile in reach 1 of Conowingo Reservoir on September 1st, 1972 at 24 hours.

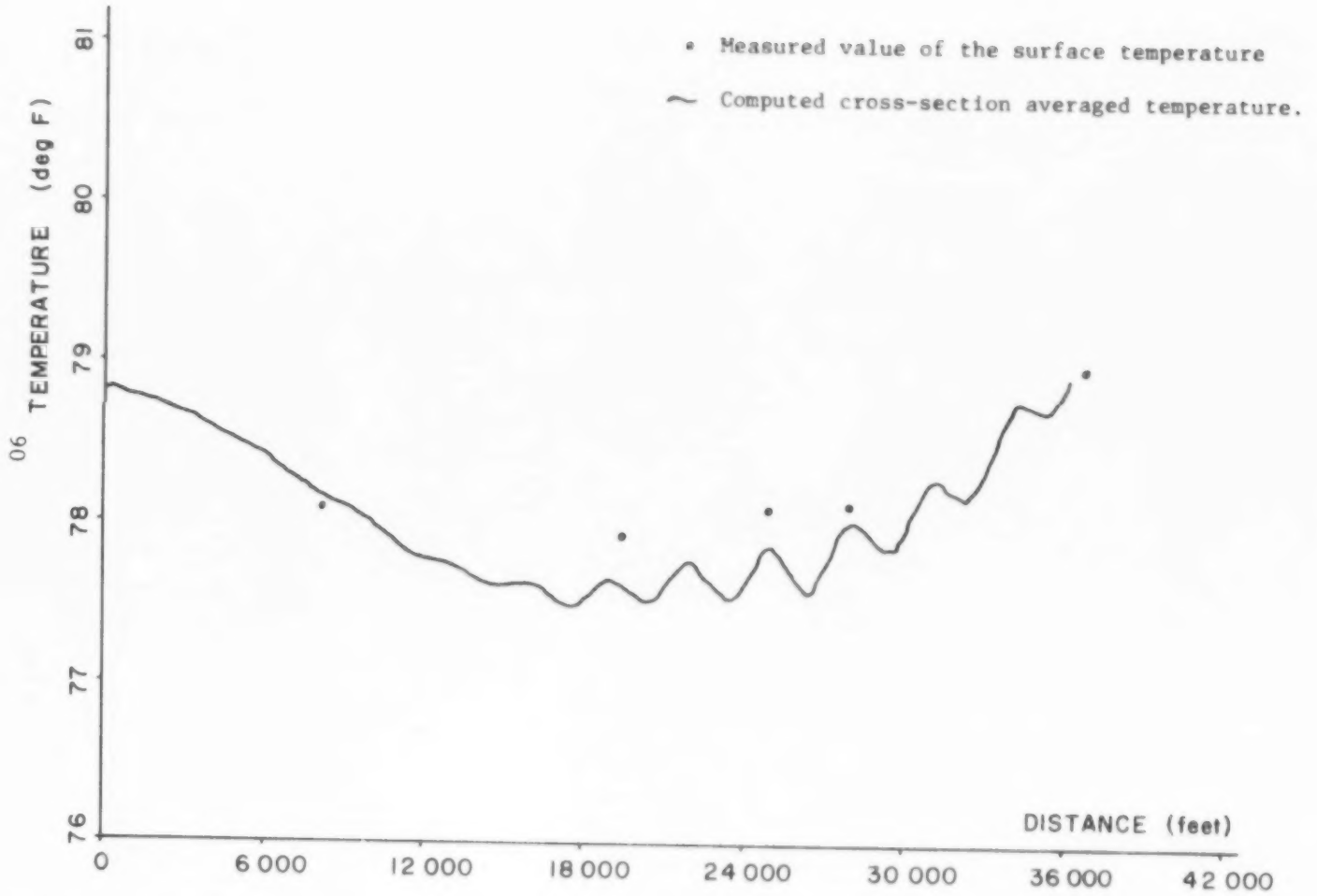

Figure 5-7: Temperature profile in reach 1 of Conowingo Reservoir on September 2nd, 1972 at 24 hours with $E_L = 100\ E_T$.

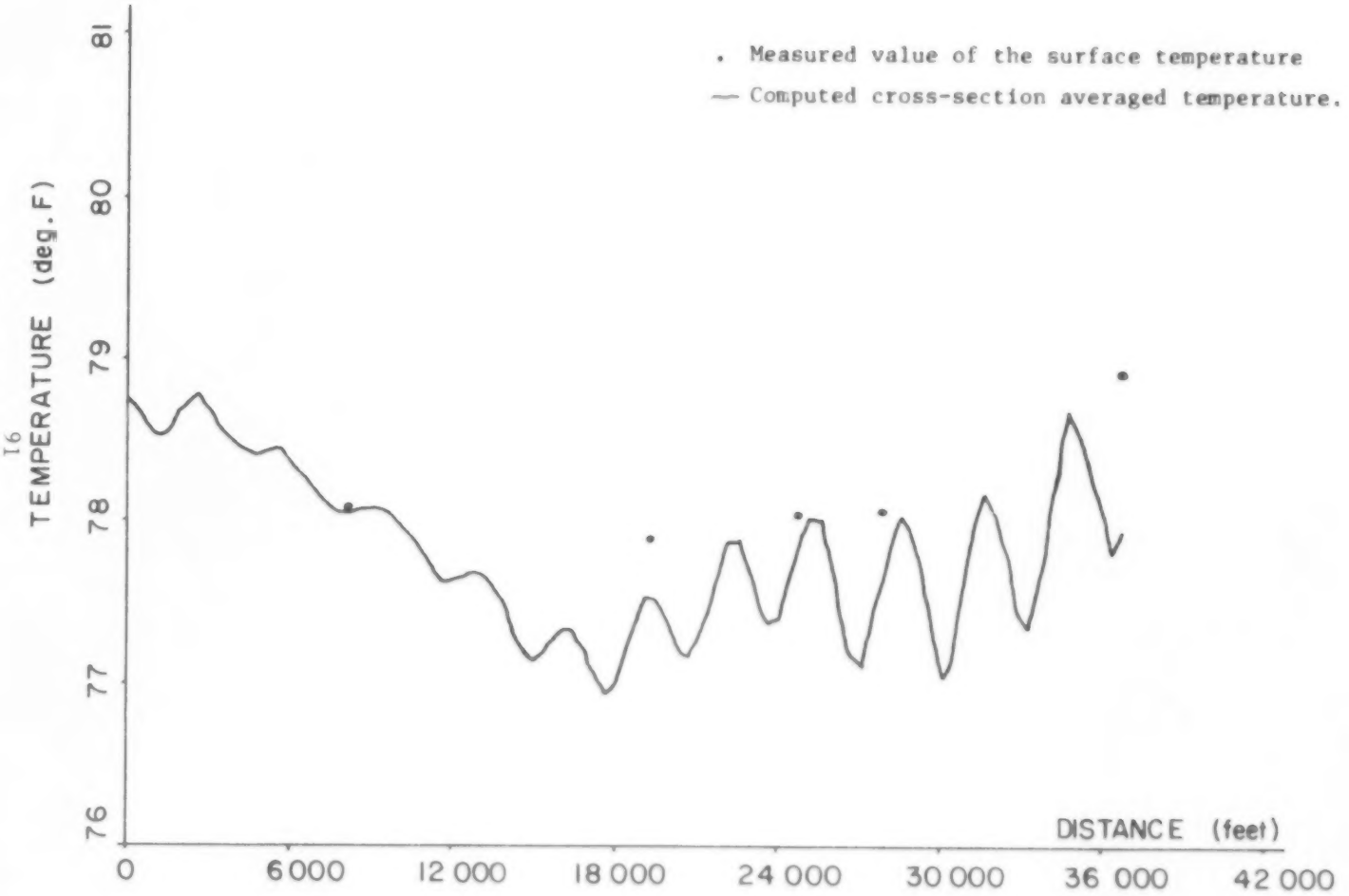

Figure 5-8: Temperature profile in reach 1 of the Conowingo Reservoir on September 2nd, 1972 at 24 hours with $E_L = 10\ E_T$.

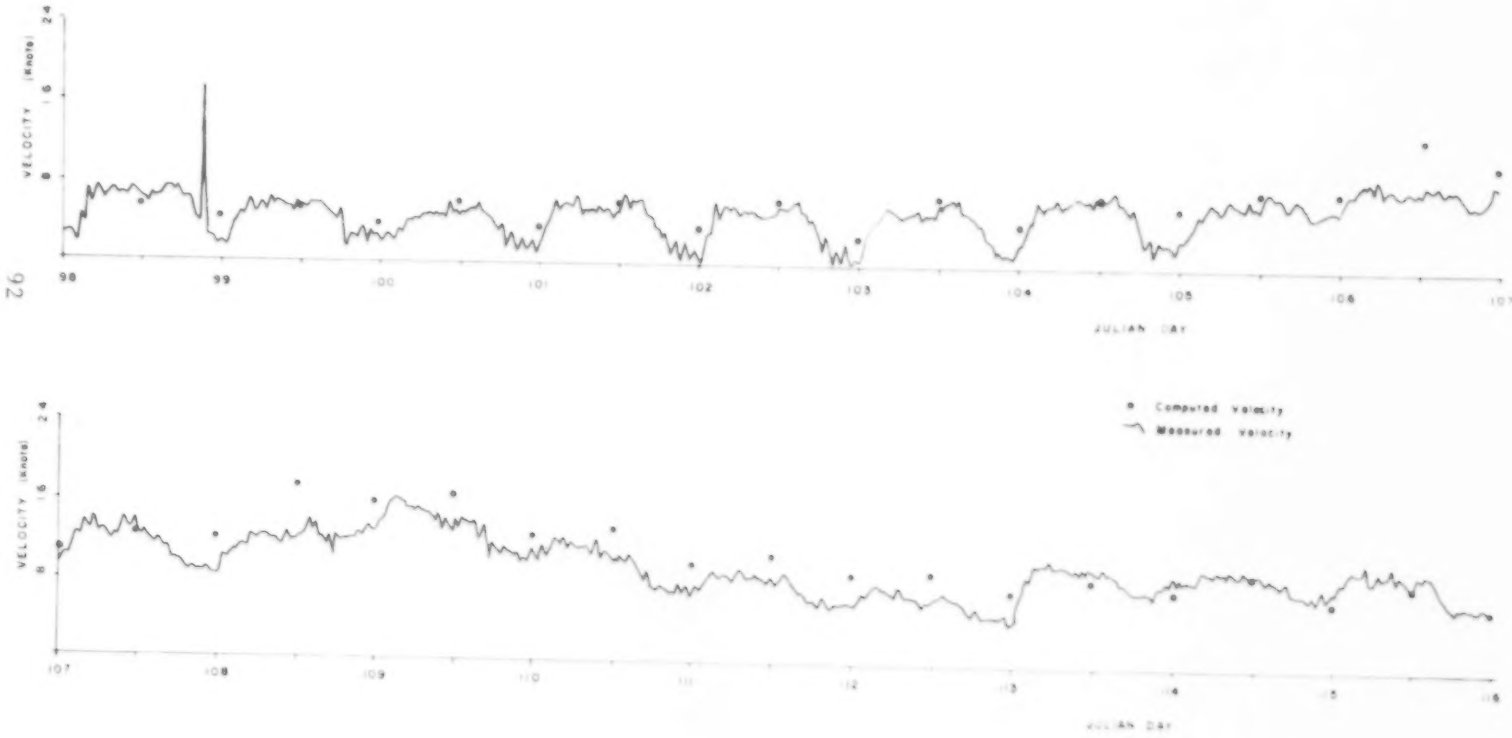

Figure 5-9: Time variations of the velocity from April 8 to 25, 1972 at x = 13,000 ft. in Conowingo Reservoir.

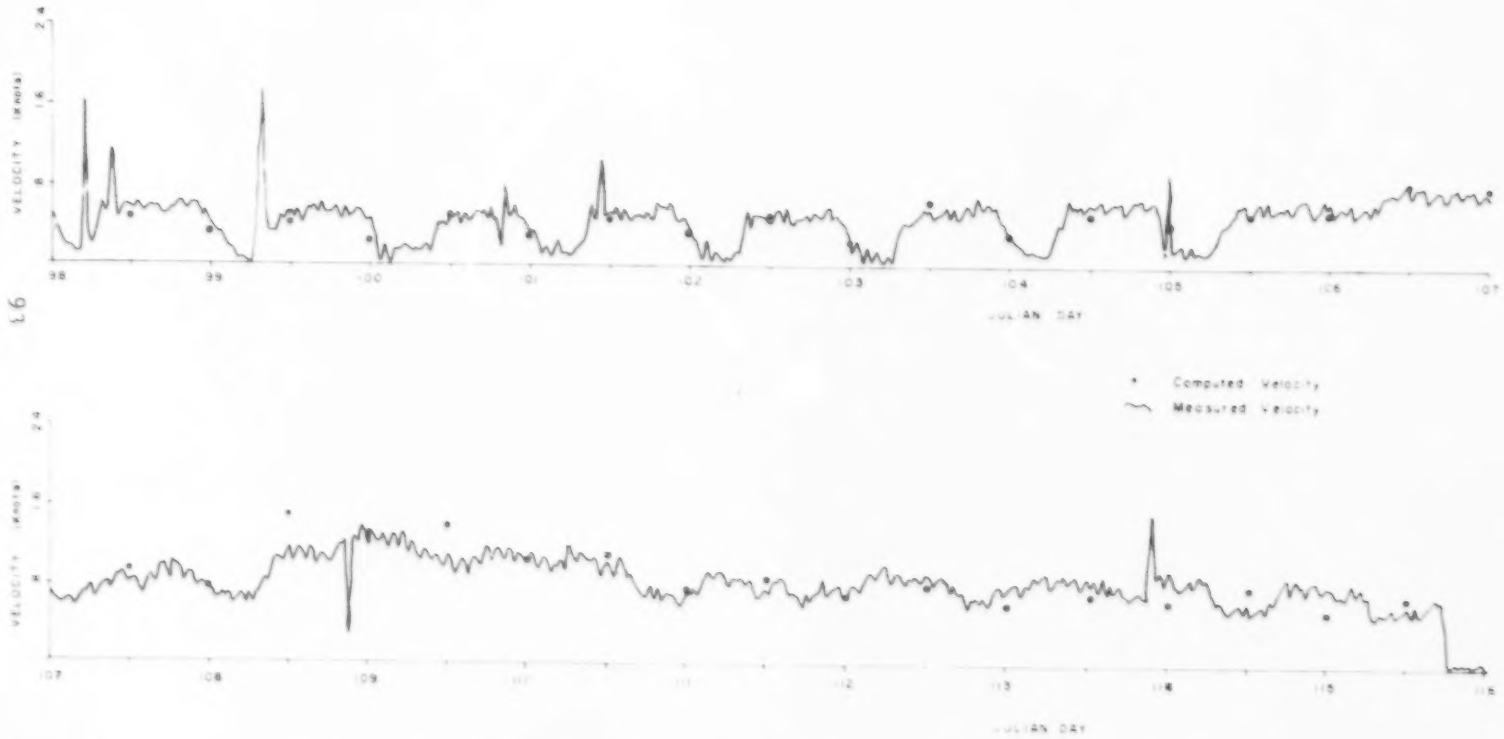

Figure 5-10: Time variations of the velocity from April 8 to 25, 1972 at x = 25,000 ft in Conowingo Reservoir.

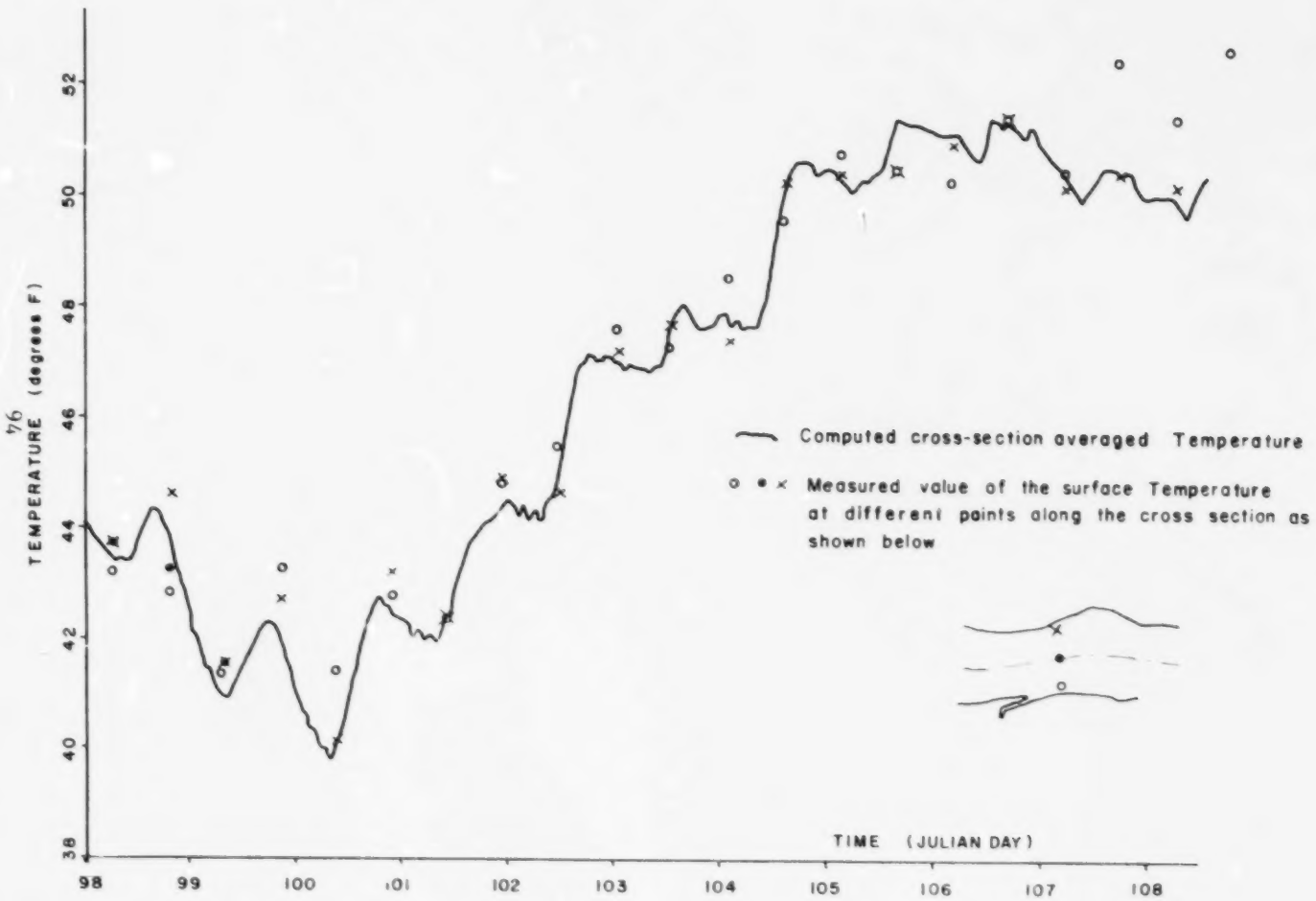

Figure 5-11: Time variations of the temperature from April 8 to 18, 1972 at x = 25,000 ft in Conowingo Reservoir.

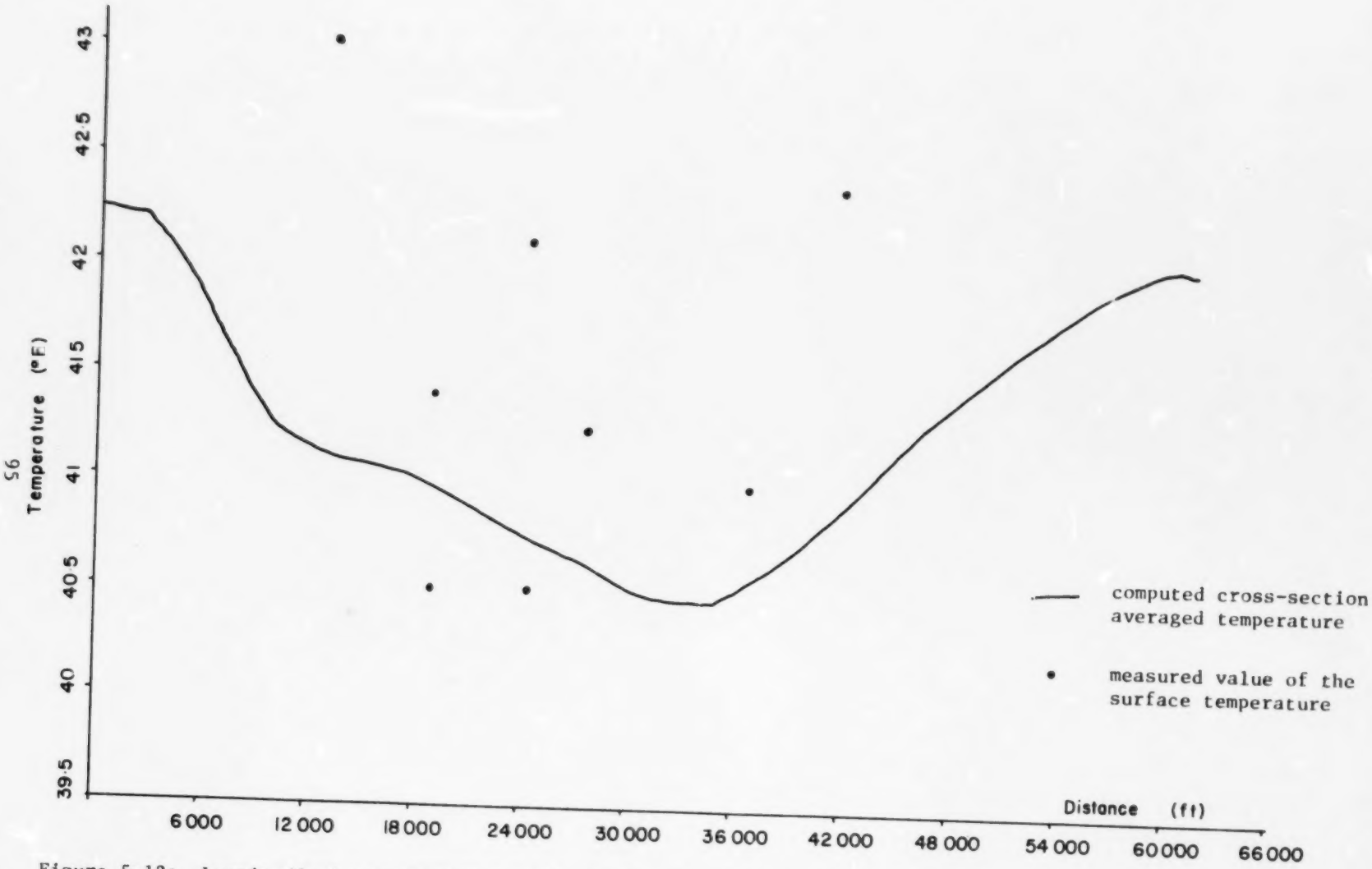

Figure 5-12: Longitudinal temperature profile in Conowingo Reservoir on April 10, 1972 at 12 hours.

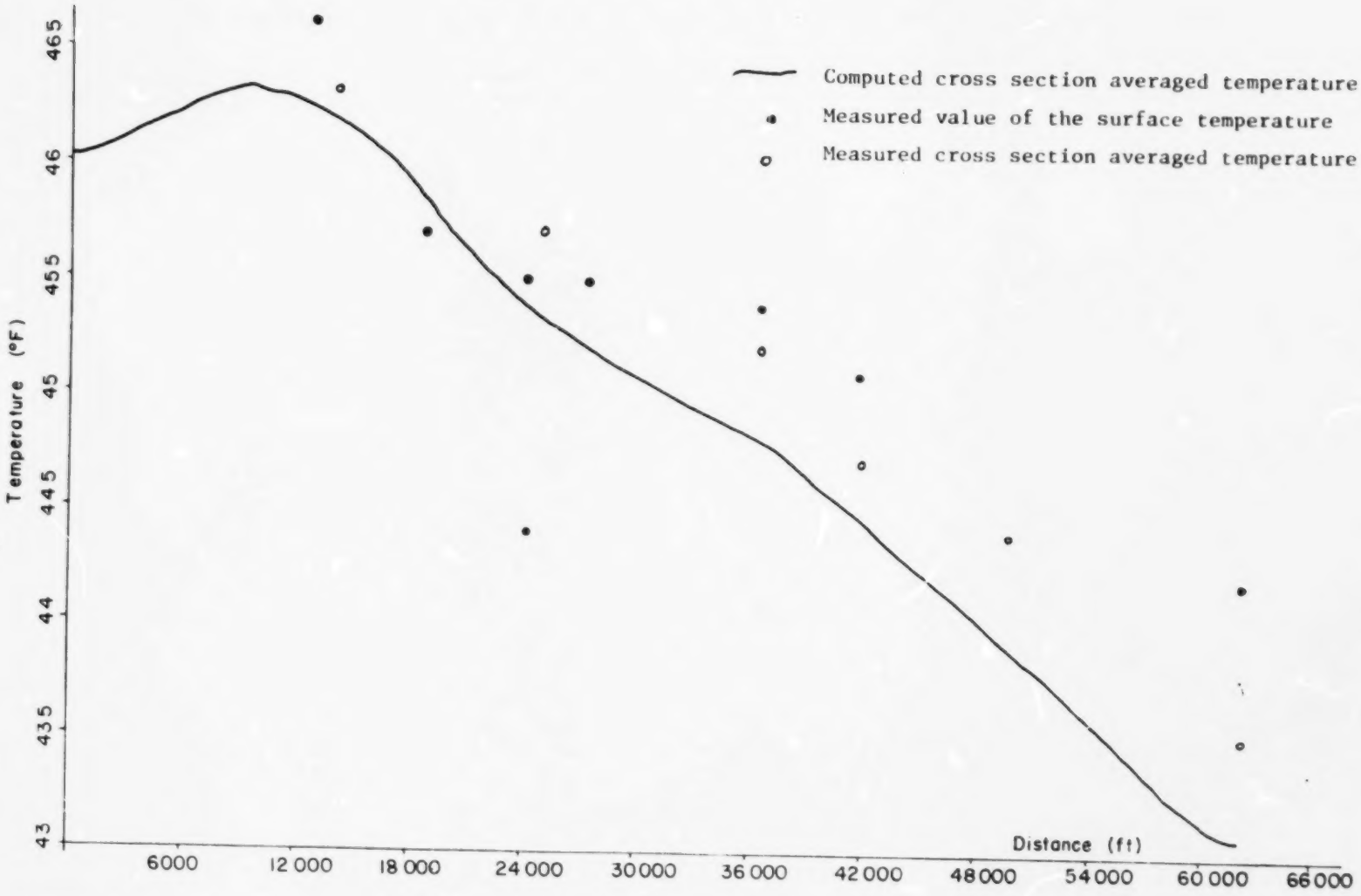

Figure 5-13: Temperature profile in Conowingo Reservoir on April 12, 1972 at 12 hours.

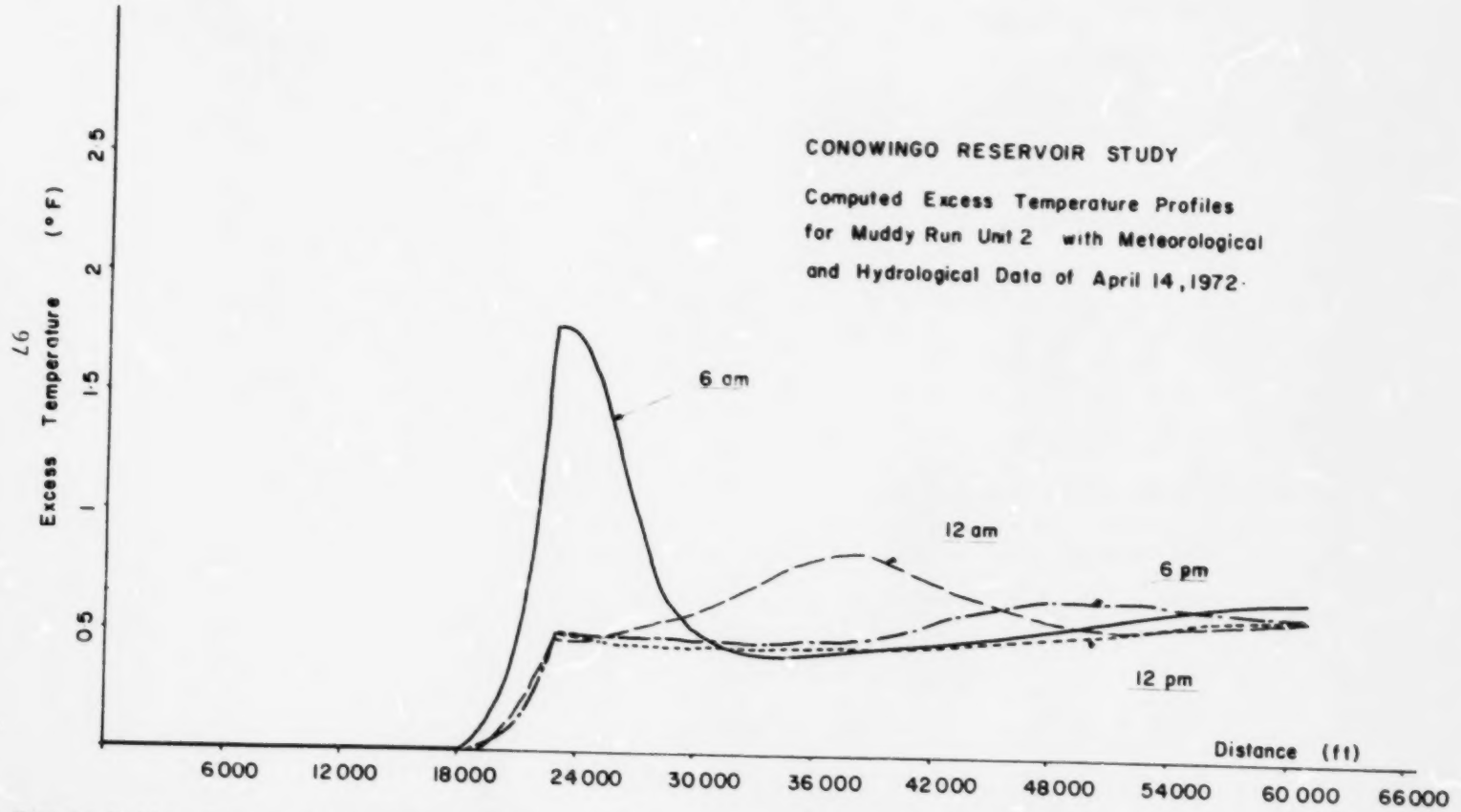

Figure 5-14: Computed excess temperature profiles in the Conowingo Reservoir due to Peach Bottom - Unit 2 with meteorological and hydrological data of April 14, 1972.

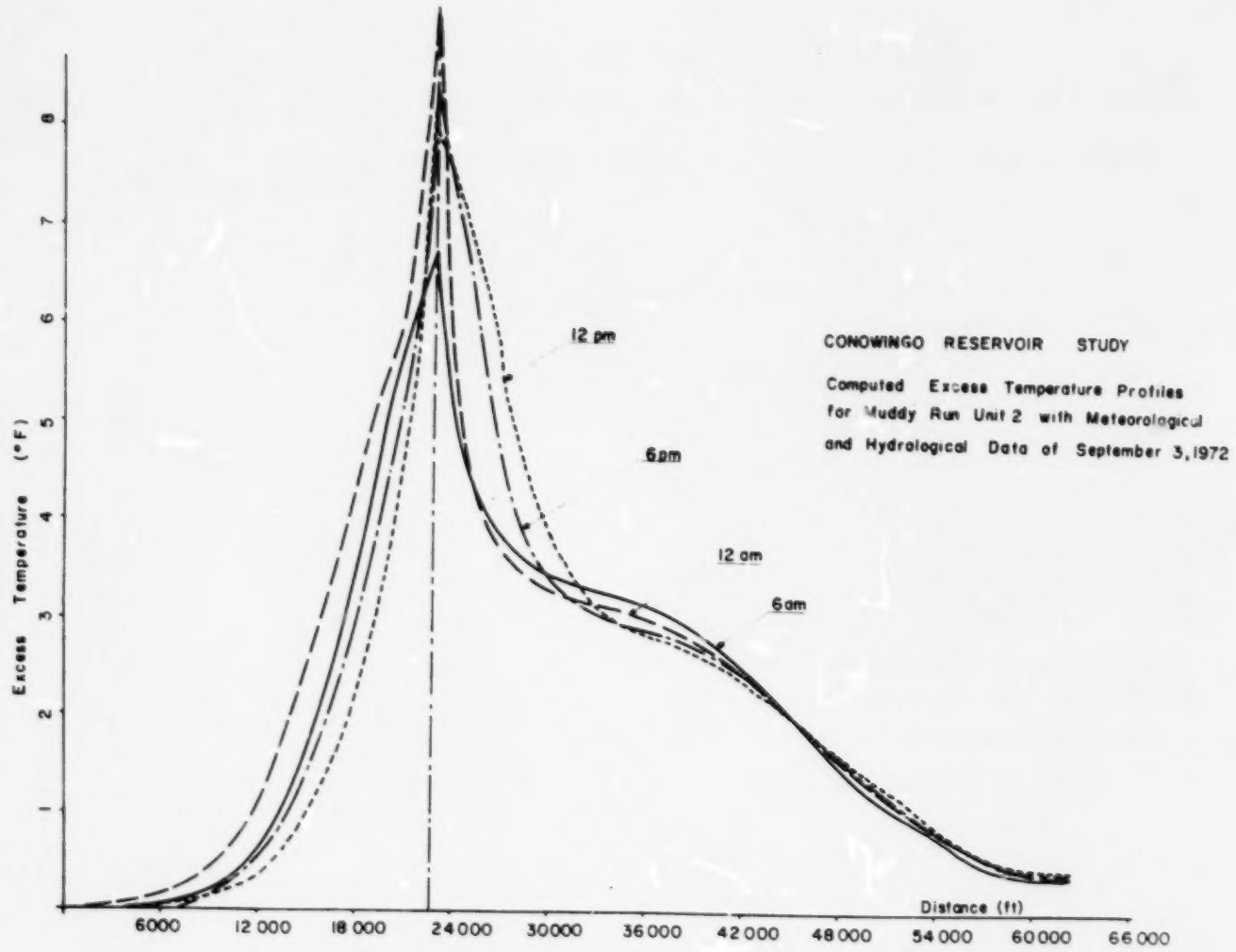

Figure 5-15: Computed excess temperature profiles in the Conowingo Reservoir due to Peach Bottom - Unit 2 with meteorological and hydrological data of September 3, 1972.

VI. CONCLUSION

The two mathematical models presented in this study allow the determination and prediction of steady and unsteady temperature distribution in free surface bodies of water where the assumptions required by a one-dimensional model can be applied. These models have been verified by comparison with analytical solutions and good agreement was found.

The data requirement for both models are geometric data, boundary conditions for the determination of the flow characteristics and meteorological conditions. In the case of the unsteady model, time variations of this data can be specified, when applicable. This requirement is sometimes difficult to meet, especially for the variations of meteorological conditions where the number of parameters to be specified is important and where long term predictions remain mostly qualitative. In that case, average seasonnal values should be used taking into account the daily variations of the solar flux and ambient temperature.

Utilization of the unsteady model is recommended in cases where the flow characteristics are highly transient, such as in estuaries or hydroelectric reservoirs and for situations in which the time variations of the meteorological conditions are to be considered. When the flow is subject only to long term variations of small amplitude, such as in rivers, the steady model presented here can give a very good first approximation and has the advantage of a lower operation cost.

The unsteady model was applied to compute natural temperature distributions in Conowingo Reservoir under time varying flows and meteorological conditions. Good correlation was obtained between the results of the model and measurements. Calculations of excess temperatures in the

reservoir with heat addition (from Peach Bottom Unit No. 2) were made under the hypothetical condition that the condenser water discharge is uniformly mixed over the cross-section of the reservoir adjacent to the power plant discharge.

REFERENCES

1. Dailey, J.E. and Harleman, D.R.F., "Numerical Model for the Prediction of Transient Water Quality in Estuary Networks", Technical Report No. 158, R. M. Parsons Laboratory for Water Resources and Hydrodynamics, Department of Civil Engineering, M.I.T., October 1972.

2. Ryan, P.J. and Harleman, D.R.F., "An Analytical and Experimental Study of Transient Cooling Pond Behavior", Technical Report No. 161, R. M. Parsons Laboratory for Water Resources and Hydrodynamics, Department of Civil Engineering, M.I.T., January 1973.

3. Eagleson, P.S., Dynamic Hydrology, McGraw-Hill Book Co., 1970.

4. Jobson, H.E., "The Dissipation of Excess Heat from Water Systems", ASCE (Journal of the Power Division), May 1973.

APPENDIX A

SUMMARY OF INTEGRAL VALUES IN THE WEIGHTED RESIDUAL EQUATIONS

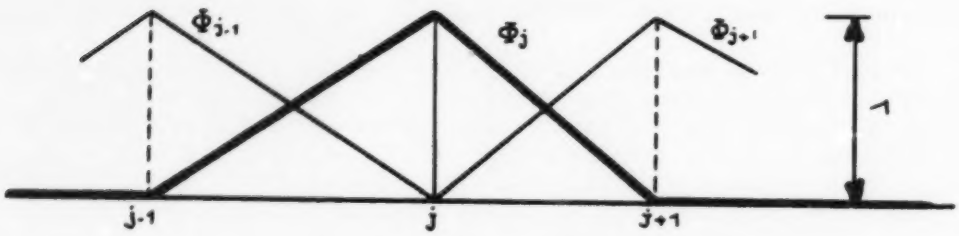

In Element j-1,j:

$$\phi_{j-1} = \frac{x_j - x}{\Delta_{j-1,j}}$$

$$\phi_j = \frac{-x_{j-1} + x}{\Delta_{j-1,j}}$$

$$\phi_{j+1} = 0$$

In Element j,j+1:

$$\phi_{j-1} = 0$$

$$\phi_j = \frac{x_{j+1} - x}{\Delta_{j,j+1}}$$

$$\phi_{j+1} = \frac{-x_j + x}{\Delta_{j,j+1}}$$

Only in elements j-1,j and j,j+1 will integrals containing ϕ_j provide a non-zero contribution. Their values are as follows:

$$\sum_E \int \frac{d\phi_j}{dx} \frac{d\phi_{j-1}}{dx} dx = -\frac{1}{\Delta_{j-1,j}}$$

$$\sum_E \int \frac{d\phi_j}{dx} \frac{d\phi_j}{dx} dx = \frac{1}{\Delta_{j-1,j}} + \frac{1}{\Delta_{j,j+1}}$$

$$\sum_E \int \frac{d\phi_j}{dx} \frac{d\phi_{j+1}}{dx} dx = -\frac{1}{\Delta_{j,j+1}}$$

$$\sum_E \int \phi_j \frac{d\phi_{j-1}}{dx} dx = -\frac{1}{2}$$

$$\sum_E \int \phi_j \frac{d\phi_j}{dx} dx = 0$$

$$\sum_E \int \phi_j \frac{d\phi_{j+1}}{dx} dx = \frac{1}{2}$$

$$\sum_E \int \frac{d\phi_j}{dx} \phi_{j-1} dx = \frac{1}{2}$$

$$\sum_E \int \frac{d\phi_j}{dx} \phi_{j+1} dx = -\frac{1}{2}$$

$$\sum_E \int \phi_j \phi_{j-1} dx = \frac{\Delta_{j-1,j}}{6}$$

$$\sum_E \int \phi_j \phi_j dx = \frac{\Delta_{j-1,j}}{3} + \frac{\Delta_{j,j+1}}{3}$$

$$\sum_E \int \phi_j \phi_{j+1} dx = \frac{\Delta_{j,j+1}}{6}$$